AD-A083 447 NAVAL SURFACE WEAPONS CENTER SILVER SPRING MD F/G 20/4
AN INTEGRAL METHOD AND ITS APPLICATION TO SOME THREE-DIMENSIONA--ETC(U)
JUL 79 T F ZIEN
UNCLASSIFIED NSWC/TR-79-139 NL

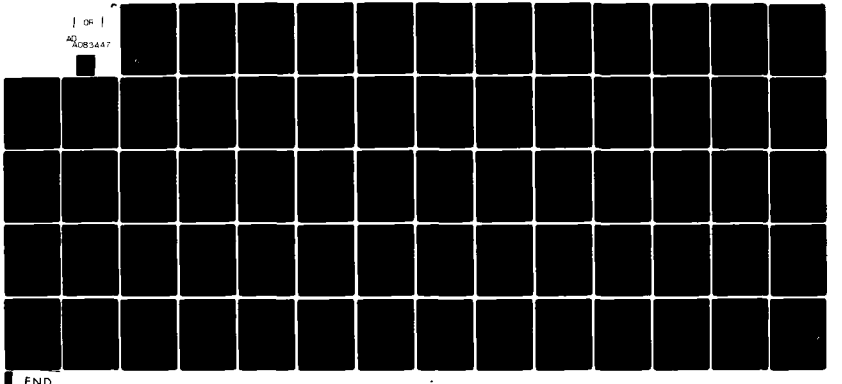

END
DATE FILMED
5-80
DTIC

NSWC TR 79-139

AN INTEGRAL METHOD AND ITS APPLICATION TO SOME THREE-DIMENSIONAL BOUNDARY-LAYER FLOWS

BY T. F. ZIEN

RESEARCH AND TECHNOLOGY DEPARTMENT

18 JULY 1979

NAVAL SURFACE WEAPONS CENTER

Dahlgren, Virginia 22448 • Silver Spring, Maryland 20910

UNCLASSIFIED

SECURITY CLASSIFICATION OF THIS PAGE *(When Data Entered)*

REPORT DOCUMENTATION PAGE

READ INSTRUCTIONS BEFORE COMPLETING FORM

1. REPORT NUMBER: NSWC/TR-79-139	2. GOVT ACCESSION NO.: AD-A083 447
3. RECIPIENT'S CATALOG NUMBER	
4. TITLE *(and Subtitle)*: AN INTEGRAL METHOD AND ITS APPLICATION TO SOME THREE-DIMENSIONAL BOUNDARY-LAYER FLOWS	5. TYPE OF REPORT & PERIOD COVERED
	6. PERFORMING ORG. REPORT NUMBER
7. AUTHOR(s): T. F. Zien	8. CONTRACT OR GRANT NUMBER(s)
9. PERFORMING ORGANIZATION NAME AND ADDRESS: Naval Surface Weapons Center, White Oak, Silver Spring, Maryland 20910	10. PROGRAM ELEMENT, PROJECT, TASK AREA & WORK UNIT NUMBERS: 61152N; ZR0000; ZR0140201; R0103
11. CONTROLLING OFFICE NAME AND ADDRESS	12. REPORT DATE: 18 July 1979
	13. NUMBER OF PAGES: 65
14. MONITORING AGENCY NAME & ADDRESS *(if different from Controlling Office)*	15. SECURITY CLASS. *(of this report)*: Unclassified
	15a. DECLASSIFICATION/DOWNGRADING SCHEDULE

16. DISTRIBUTION STATEMENT *(of this Report)*

Approved for public release, distribution unlimited

17. DISTRIBUTION STATEMENT *(of the abstract entered in Block 20, if different from Report)*

18. SUPPLEMENTARY NOTES

19. KEY WORDS *(Continue on reverse side if necessary and identify by block number)*

Mathematical Methods, Approximation Methods, Viscous Boundary Layers, Three-Dimensional Boundary Layers

20. ABSTRACT *(Continue on reverse side if necessary and identify by block number)*

The simple integral method developed and successfully employed by the author to provide accurate approximate solutions to a wide variety of problems in viscous boundary-layer flows and transient heat conduction with phase changes is further studied. A simple boundary value problem in ordinary differential equation is used as the model problem for the study. Different schemes of the method used in earlier applications are examined in

DD FORM 1 JAN 73 1473 EDITION OF 1 NOV 65 IS OBSOLETE
S/N 0102-014-6601

UNCLASSIFIED
SECURITY CLASSIFICATION OF THIS PAGE *(When Data Entered)*

some detail along with a new and potentially more accurate scheme. On the basis of the comparison between the approximate solutions and the exact solution, some remarks on the relative merits of the various schemes are made along with some observations on the judicious choice of the approximate profiles for use in the calculation. The method is then applied to yield approximate solutions of a class of relatively simple three-dimensional boundary-layer flows. Results are reported of boundary layers on a semi-infinite flat plate with parabolic and circular inviscid surface streamlines, and boundary layers over an infinite yawed wing. Results are presented in terms of skin-friction, and are all obtained in simple closed form. Comparisons with existing exact solutions are included to indicate the accuracy of the method.

SUMMARY

This report contains results of a study of the new integral method developed at the Naval Surface Weapons Center (NAVSWC), and its application to three-dimensional boundary-layer calculations. The work is a part of a theoretical study of general viscous flow problems. The study is supported by NAVSWC Independent Research Program.

Paul R. Wessel

PAUL R. WESSEL
By direction

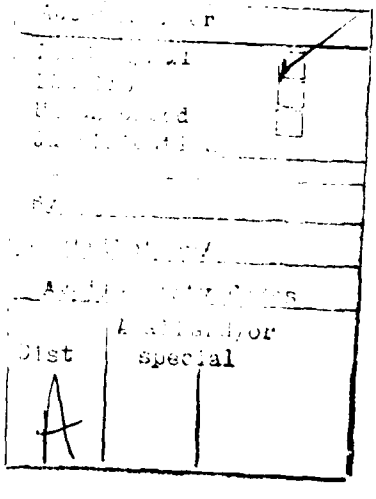

CONTENTS

ILLUSTRATIONS

1. INTRODUCTION

The simple integral method developed by the author has been extensively used to provide approximate solutions to a wide variety of problems in two-dimensional laminar boundary-layer flows[1,2] and transient heat conduction with phase transition[3,4]. More recently, application of the method was made by King[5] to give a simple, yet accurate, prediction of the critical Reynolds number for a heated flat plate in water in connection with the boundary-layer stability studies.

In the previous development and application of the method, various different schemes[3] based on the same basic idea have been proposed and used for the approximate solutions of the different problems mentioned above. Also, different forms of the approximate profile with a varying degree of complexity were assumed in the calculation process, and the dependence of the approximate solution on the assumed profile has been noted and discussed. While the results obtained so far are all favorable and only weakly dependent on the profiles, the limit of the capability of the method in accommodating improper profiles has not been studied before, and the relative merit of the various schemes for a given problem remains to be determined. From a practical standpoint, some guidelines in choosing an approximate profile based on the given boundary conditions and the governing differential equations are very helpful in achieving good results, and a systematic approach in developing such guidelines appears desirable.

In this report, a study of the method related to the aforementioned questions is made in section 2. A simple boundary value problem in ordinary differential equation is used as a model example for the study. Two approximate profiles of polynomial form are used in conjunction with every different scheme of the integral method. Corresponding solutions are then compared with the exact solution so as to determine their accuracy. The qualitative behavior of the exact solution is also deduced from the differential equation and the given boundary conditions, and is used to establish certain guidelines for choosing the most appropriate solution in cases where multiple solutions are generated in the solution process of certain schemes.

The integral method is next used to yield approximate solutions to some simple three-dimensional boundary-layer flows in section 3; only laminar incompressible

1. Zien, T. F., "A New Integral Calculation of Skin Friction on a Porous Plate," AIAA Journal, Vol. 9, No. 7, Jul 1971, pp. 1423-1425.
2. Zien, T. F., "Approximate Analysis of Heat Transfer in Transpired Boundary Layer with Effects of Prandtl Number," International Journal of Heat and Mass Transfer, Vol. 19, No. 5, May 1976, pp. 513-521.
3. Zien, T. F., "Study of Heat Conduction with Phase Transition Using an Integral Method," AIAA Progress in Astronautics and Aeronautics, Vol. 56, Thermophysics of Spacecraft and Outer Planet Entry Probes (Ed. A. M. Smith), Sep 1977, pp. 87-111.
4. Zien, T. F., "Integral Solutions of Ablation Problems with Time-Dependent Heat Flux," AIAA Journal, Vol. 16, No. 12, Dec 1978, pp. 1287-1295.
5. King, W. S., "An Approximate Method for Estimating the Critical Reynolds Number for a Heated Flat Plate in Water," Rand Paper Series P-6176, The Rand Corporation, Santa Monica, Calif., Aug 1978.

flows are considered. Examples include flat-plate boundary layers with parabolic inviscid streamlines, boundary layers over yawed wedges and boundary layers on a flat plate with circular inviscid streamlines and small turning angles. These flows all have the common feature that one lateral velocity component is decoupled from the other. This simplifies the solution process considerably, and allows closed-form solutions to be obtained for all the cases treated in the report. Solutions are presented mainly in terms of skin friction components. Mathematically speaking, the system of governing equations resembles that pertaining to heat transfer problems in two-dimensional boundary-layer flows.

Finally in section 4, some remarks are made about the method in general, and its application to three-dimensional boundary-layer flows in particular.

2. THE INTEGRAL METHOD--A MODEL EXAMPLE

The basic idea of the integral method discussed here lies in the use of the integrated version of the differential equation as an expression for the boundary derivatives, after an approximate (guess) solution is substituted for the (unknown) exact solution in the various integrals. In application to physical problems, the boundary derivatives are often related to the important quantities of surface flux, e.g., skin friction (momentum flux), heating rate (heat flux), etc. on an aerodynamic body, and their accurate and efficient predictions are of great importance in the design and performance analysis of the body.

In this report, the basic idea of the method is exhibited in an elementary manner by way of a simple boundary value problem in ordinary differential equation, and examined in some detail from a mathematical viewpoint. Although this model example does not simulate the mathematical structure of the physical problems intended for the application of the method, it is thought to be capable of allowing the central idea to be presented with ease and clarity without being obscured by mathematical complexities.

2.1 EXACT SOLUTION.

Consider the following problem:

$$\frac{d^2y}{dx^2} = y \qquad 0 \le x \le 1 \tag{1.1}$$

$$y(0) = 0 \tag{1.2a}$$

$$y(1) = 1 \tag{1.2b}$$

The exact solution is easily obtained as

$$y = \sinh x/\sinh 1 \tag{1.3a}$$

whereby the boundary derivatives can be evaluated as

$$(dy/dx)_0 = 0.8509; \quad (dy/dx)_1 = 1.3130 \tag{1.3b}$$

These exact results will be used later as a standard to determine the accuracy of various approximate solutions to be generated.

To discuss the qualitative behavior of the exact solution on the basis of the differential equation and the given boundary conditions alone, we may proceed as follows. First, rewrite Eq. (1) as the following pair of equations

$$\frac{dy}{dx} = z \tag{1.4a}$$

$$\frac{dz}{dx} = y \tag{1.4b}$$

from which the following equation for the slope, z, results

$$\frac{dz}{dy} = \frac{y}{z} \tag{1.5}$$

Eq. (1.5) is integrated to provide information about the slope of the solution curve,

$$z^2 = y^2 + c \tag{1.6}$$

where c is an integration constant. Eq. (1.6) represents families of hyperbolas in (y,z) plane with the axis either aligned with the y-axis (I, for $c < 0$) or with the z-axis (II, for $c > 0$) (see Fig. 1). Since the solution domain extends to $y = 0$, viz., $0 \le y \le 1$, family I must be excluded from consideration. In family II, only the segments in $y > 0$ are relevant to the desired solution in view of the specified domain of solution, $0 \le y \le 1$. Finally, the solution branch is determined as labeled in Fig. 1 on the basis that z (= dy/dx) must be at least positive in a finite region of y within $1 \le y \le 1$, to accommodate the boundary conditions of y increasing from 0 to 1 while x increasing from 0 to 1.

Based on the above discussion, some important properties of the solution can be deduced, and are listed in the following for use in determining a profile in the approximate solution:

(i) $y(x) > 0$ in $0 < x \le 1$
(ii) $y'(x)$, particularly $y'(0)$, is positive in $0 \le x \le 1$
(iii) $y''(1) > 0$ (because $y''(1) = y(1) = 1$ from Eqs. (1.1) and (1.2b))

In deciding the desired solution for the profile parameter in case of multiple solutions in certain solution schemes, the above listed properties will be used as a guideline. This approach is also suggested for the application of the method to other physical problems.

One way to construct profiles as approximate solutions to the problem is to use polynomials which are formed to satisfy the given boundary conditions, and satisfy the differential equation in an averaged sense, but not locally. Two such polynomials are given below and will be used in the various approximate solution schemes.

$$f_1 = Ax + (1-A)x^2 \tag{1.7}$$

$$f_2 = Ax^2 + (1-A)x^3 \tag{1.8}$$

In these profiles, A is a constant profile parameter to be determined. The cubic polynomial, f_2, is obviously ill-chosen because it gives zero slope at $x = 0$. It is included here to test if reasonable solutions of the boundary derivatives can be achieved with the present integral method even if the assumed profile is an improper one.

The properties (i), (ii) and (iii) of the exact solution as enumerated above can now be used to establish certain conditions to be imposed on the profile parameter A for such polynomial profiles. For example,

(i) leads to $A > 0$ for both f_1 and f_2,

(ii) leads to $A < 2$ for f_1
and $A < 3$ for f_2

(iii) leads to $A < 1$ for f_1
and $A < 1.5$ for f_2

The above conditions can be summarized as

$$f_1 : 0 < A < 1 \tag{1.9}$$

$$f_2 : 0 < A < 1.5 \tag{1.10}$$

Eqs. (1.9) and (1.10) will be considered to be the desirable ranges of the solution of A.

2.2 CLASSICAL INTEGRAL METHOD. The simplest kind of the integral method makes use of the integrated form of the original differential equation alone, and the idea is the same as that of the well-known Karman-Pohlhausen momentum integral technique for solving boundary-layer flow problems.

A direct integration of the differential equation, (1.1), gives

$$\left(\frac{dv}{dx}\right)_1 - \left(\frac{dy}{dx}\right)_0 = \int_0^1 y\,dx \tag{1.11}$$

In the classical integral method, y is replaced by f, the assumed profile, in all terms of Eq. (1.11), including both derivatives and integrals. Thus

$$\left(\frac{df}{dx}\right)_1 - \left(\frac{df}{dx}\right)_0 = \int_0^1 f\,dx \tag{1.12}$$

(i) $f = f_1$: Eq. (1.12) gives the following solution:

$$A = \frac{10}{13} ;$$

$$\left(\frac{dy}{dx}\right)_0 = A = 0.7692 \ (-9.6\%)$$

$$\left(\frac{dy}{dx}\right)_1 = 2\text{-}A = 1.2308 \ (-6.3\%)$$

Here, and in all the following results, the percentage errors are indicated in the parenthesis.

(ii) $f = f_2$: Eq. (1.12) for this case leads to the following solution:

$$A = \frac{33}{13} = 2.5385$$

$$\left(\frac{dy}{dx}\right)_0 = 0 \ (-100\%)$$

$$\left(\frac{dy}{dx}\right)_1 = 3\text{-}A = 0.4615 \ (-64.9\%)$$

It is noted here that this purposely ill-chosen profile, f_2, indeed leads to unacceptable accuracy in the boundary derivative predictions.

In the following, the same profiles will be used in conjunction with the new integral method, and improved accuracies will be demonstrated which indicate the potential of the present method in, among other things, tolerating improper profiles.

2.3 PRESENT INTEGRAL METHOD. As a refinement of the classical integral method, various moment equations are generated from the original differential equation and used in conjunction with the directly integrated form of the original equation. This way the boundary derivatives can be expressed in terms of the integrals involving the approximate profile (assumed) via the integrated equation, Eq. (1.11). This idea forms the basis of the present integral method.

Depending on how the moment equations are generated, the present integral method further divides itself into various different schemes which will be described in the following.

2.3.1 x-Moment Scheme. In this scheme, the additional equation is generated as follows,

$$\int_0^1 x \frac{d^2y}{dx^2} dx = \int_0^1 xydx \qquad (1.13)$$

which reduces to

$$\left(\frac{dy}{dx}\right)_1 - 1 = \int_0^1 xy\,dx \tag{1.14}$$

where the boundary conditions, Eqs. (1.2a,b), have been used.

Eqs. (1.11) and (1.14) form the basic system of equations for the solution of the boundary derivatives, y'(1) and y'(0), and the parameter A. f will be substituted for y only in the integrals of Eqs. (1.11) and (1.14). Some assumptions regarding either y'(0) or y'(1) will be required for a solution.

(i) y'(1) = f'(1).

In this case, we have two equations for the two unknowns, y'(0) and A, after f is substituted for y inside the integrals. The solutions are summarized below

(a) $f = f_1$: A = 0.6923,
y'(0) = 0.8589 (+0.9%)
y'(1) = 1.3077 (-0.4%)

(b) $f = f_2$: A = 1.7143
y'(0) = 0.8929 (+4.9%)
y'(1) = 1.2857 (-2.1%)

Note that in view of the discussion in §2.1, the solution of A corresponding to f_2 falls somewhat beyond the range specified in Eq. (1.10). However, this solution is still used here because there is no other solution available in this scheme. It perhaps should be remarked that the relatively large errors of this solution may well be a result of this difficulty. Nevertheless, the solution is still much more accurate than the classical integral solution corresponding to the same profile.

(ii) y'(0) = f'(0).

In this case, the two equations, (1.11) and (1.14), are used to determine y'(1) and A. Only f_1 is appropriate for this calculation, as $f_2'(0) = 0$ which in turn leads to y'(0) = 0 in this case. This obviously incorrect result (see discussion on the qualitative behavior of the exact solution in §2.1) should be avoided, if possible.

For $f = f_1$, the results are summarized below:

$$A = \frac{11}{13} = 0.8462$$

$$y'(0) = 0.8462 \ (-0.6\%)$$

$$y'(1) = \frac{7}{6}A + \frac{1}{3} = 1.3205 \ (+0.6\%)$$

The accuracy is seen to be equally good as in case (i).

2.3.2 y-Moment Scheme. In this scheme, the additional equation is obtained from the y-moment integral of the original differential equation, i.e.,

$$\int_0^1 y \frac{d^2y}{dx^2} dx = \int_0^1 y^2 dx \tag{1.15}$$

Since

$$y \frac{d^2y}{dx^2} = \frac{1}{2} \frac{d^2}{dx^2} y^2 - \left(\frac{dy}{dx}\right)^2,$$

Eq. (1.15) can be rewritten as

$$\frac{1}{2} \int_0^1 \frac{d^2}{dx^2} y^2 dx - \int_0^1 \left(\frac{dy}{dx}\right)^2 dx = \int_0^1 y^2 dx \tag{1.16}$$

It should be noted here that the y-moment scheme invariably leads to a nonlinear equation even if the original equation is linear. Also, in this scheme, a term

$$\int_0^1 \left(\frac{dy}{dx}\right)^2 dx$$

appears, and its calculation can be done in two different ways.

The simplest way is to substitute dy/dx by df/dx inside the integral, and this scheme will be referred to as the y_d-moment scheme, where "d" signifies differential expression for y'(x)

$$y_d\text{-moment scheme: } \frac{1}{2} \int_0^1 \frac{d^2}{dx^2} y^2 dx - \int_0^1 \left(\frac{df}{dx}\right)^2 dx = \int_0^1 f^2 dx \tag{1.17}$$

The other way which is perhaps more consistent with the basic idea of the method is to obtain an integral expression for dy/dx from an integration of the original differential equation, i.e.,

$$\frac{dy}{dx} = \left(\frac{dy}{dx}\right)_1 - \int_x^1 y dx \tag{1.18}$$

If we now assume y'(1) = f'(1), this scheme which will be referred to as the y_i-moment scheme ("i" signifies integral expression for y'(x)) makes use of the following equation

$$\frac{1}{2} \int_0^1 \frac{d^2}{dx^2} y^2 dx - \int_0^1 \left[f'(1) - \int_x^1 f(x) dx\right]^2 dx = \int_0^1 f^2 dx \tag{1.19}$$

It is important to note that the y_i-moment scheme couples the two basic equations, (1.11) and (1.16) in determining the solution of A whereas the y_d-moment scheme determines the solution of A by Eq. (1.16) alone.

In the following, y_d- and y_i-moment schemes will be used separately, but $y'(1) = f'(1)$ is assumed in all calculations.

(i) y_d-moment Scheme

Eq. (1.11) gives

$$y'(0) = f'(1) - \int_0^1 f dx, \tag{1.20a}$$

and Eq. (1.17) gives

$$f'(1) - \int_0^1 f'^2(x)dx = \int_0^1 f^2(x)dx \tag{1.20b}$$

(a) $f = f_1$

Letting $f = f_1 = Ax + (1-A)x^2$, we get from Eq. (1.20b) the solution of A as

$$A = 0.6826$$

where the other solution $A = -1.8644$ has been disregarded in view of Eq. (1.9). Eq. (1.20a) then gives

$$y'(0) = 0.8703 \ (+2.3\%)$$

and

$$y'(1) = f_1'(1) = 1.3174 \ (+0.3\%)$$

The accuracy is comparable to that found in §2.3.1.

(b) $f = f_2$

Eq. (1.20b) gives

$$A = 1.5725, \ -4.7058$$

Although none of the above satisfies Eq. (1.10), the solution

$$A = 1.5725$$

is chosen because it is closer to the desired range.

Eq. (1.20a) then gives

$$y'(0) = 1.0465 \ (+23\%)$$

and

$$y'(1) = 1.4275 \ (+8.7\%)$$

While the accuracy here is still better than that of the corresponding classical integral solution (§2.2, (ii), it is far less satisfactory than the accuracy of the previous results of the present method. It will be shown later that the y_1-moment scheme with the same profile will yield much improved results.

(ii) y_1-moment Scheme

Eq. (1.11) and Eq. (1.19) are the basic equations in this scheme. These equations, written explicitly, have the following forms

$$y'(0) = f'(1) - \int_0^1 f dx \tag{1.20a}$$

and

$$f'(1) - \int_0^1 [f'(1) - \int_x^1 f^2(x)dx]^2 dx = \int_0^1 f^2(x)dx \tag{1.21}$$

(a) $f = f_1$

Eq. (1.21) reduces to the following algebraic equation for A:

$$A^2 - 2.2157A + 1.0505 = 0$$

from which we have

$$A = \underline{0.6873}, \ 1.5284$$

Here, the underlined solution is obviously preferred because of Eq. (1.9). The boundary derivatives then follow immediately from Eq. (1.20a) and $y'(1) = f_1'(1)$ as

$$y'(0) = 0.8648 \ (+1.6\%)$$

and

$$y'(1) = 1.3127 \ (-0.02\%)$$

The accuracy is seen to be excellent.

(b) $f = f_2$

Here, the equation for A is, from Eq. (1.21),

$$A^2 - 4.3389A + 4.4814 = 0,$$

and

$$A = \underline{1.6949}, \ 2.6440.$$

Again, none of the above solutions falls in the desired range, Eq. (1.10), and the underlined solution is chosen because it is closer to the desired range. We then have

$$y'(0) = 0.9139 \ (+7.4\%),$$

and

$$y'(1) = 1.3051 \ (-0.6\%).$$

These results show substantial improvements on the corresponding results based on the y_i-moment scheme.

2.3.3 Combined x-Moment and y_d-Moment Scheme. A more consistent variation of the present integral method makes use of two additional equations generated by taking the x-moment and y-moment integral, respectively, of the original differential equation. The direct integral of the original differential equation is still used as the basic equation in the system. The three equations so obtained then determine the three unknowns, y'(0), y'(1) and A, and no assumptions such as y'(0) = f'(0) or y'(1) = f'(1) would be necessary.

In this section, the simpler version involving the use of the y_d-moment scheme will be discussed first. The three equations are given below:

$$\text{Direct integration:} \quad y'(1) - y'(0) = \int_0^1 f(x)dx, \tag{1.22a}$$

$$\text{x-moment integral:} \quad y'(1) - 1 = \int_0^1 xf(x)dx, \tag{1.22b}$$

and

$$y_d\text{-moment integral:} \quad y'(1) - \int_0^1 (f'(x))^2dx = \int_0^1 f^2(x)dx. \tag{1.22c}$$

Eqs. (1.22) form a system for the solution of A, y'(0) and y'(1).

(a) $f = f_1$

For this profile, the solutions of A are obtained as

$$A = \underline{0.7727}, \ 1$$

The underlined solution is used because of Eq. (1.9). The boundary derivatives corresponding to this choice of A are

$$y'(0) = 0.8523 \ (+0.2\%)$$

$$y'(1) = 1.3144 \ (+0.1\%)$$

The accuracy is found to be excellent.

(b) $f = f_2$

The use of this profile leads to the following algebraic equation for A:

$$A^2 - 4.2167A + 5.2 = 0$$

for which there is no real solution. Therefore, solution of the problem corresponding to this profile does not exist.

2.3.4 Combined x-moment and y_1-moment Scheme. In this scheme, Eq. (1.22c) is replaced by Eq. (1.21), and Eqs. (1.22a,b) and (1.21) determine the unknowns y'(0), y'(1) and A. Solutions are indicated in the following:

(a) $f = f_1$

The equation for A is

$$A^2 + 0.7243A - 1.1189 = 0$$

for which

$$A = 0.7559, -1.4802.$$

Obviously A = 0.7559 is the preferred solution in view of Eq. (1.9). The boundary derivatives are determined to be

$$y'(0) = 0.8537 \ (+0.3\%)$$

$$y'(1) = 1.3130 \ (\text{almost exact})$$

The results are seen to be almost exact.

(b) $f = f_2$

For this profile, the equation for A is

$$A^2 + 0.11832A - 5.0887 = 0$$

for which the solutions are

$$A = \underline{2.1930}, -2.3113.$$

Actually, none of the above solutions of A satisfies the requirement, Eq. (1.10). However, A = 2.1930 is used because it is the closer of the two to the desired range.

The boundary derivatives are found to be

$$y'(0) = 0.8769 \ (+3\%)$$

$$y'(1) = 1.3097 \ (-0.3\%)$$

These solutions are very accurate, in spite of the value of A being outside the desired range. In particular, the improvement in the accuracy of boundary derivatives over the previous solutions corresponding to the same profile is remarkable. This suggests that this more consistent scheme of calculation has the potential of accommodating improperly chosen profiles, and further exploration of the potential appears warranted.

2.4 REMARKS. The results of §2.2 and §2.3 clearly demonstrate the superiority of the present integral method over the classical method. For a given guess (approximate) solution, the various schemes of the present method all lead to more accurate solutions of the boundary derivatives than the classical method. The results also indicate that some understanding in the qualitative behavior of the exact solution is important and can be very helpful in determining the approximate solution. The more consistent version of the method, i.e., the combined x-moment and y-moment scheme, appears more accurate than the single moment schemes (x-moment or y-moment). However, the higher accuracy is achieved at the expense of simplicity.

In the y-moment scheme, differential and integral expressions of the term

$$\int_0^1 (dy/dx)^2 dx$$

are possible, leading, respectively, to the y_d-moment and y_i-moment schemes. It appears that the y_i-moment scheme provides more accurate results. This is significant in application to physical problems such as transient heat conduction, boundary layer flows, etc., because here a term of this kind usually exists in the original equation (e.g., the frictional heating term in thermal boundary-layer equations).

A conclusive comparison of the relative merit of the various schemes of the present integral method does not seem possible at present, because the results reported here are somewhat limited in generality. In addition, they do not seem to indicate any definitive preference of one scheme to the other. However, the combined x-moment and y-moment scheme appears to give better results, whenever results are obtainable, than the other one-moment type of schemes.

The results are mainly presented and discussed in terms of the boundary derivatives, with little emphasis on the solution in the entire region. To be sure, the primary motivation of the present modification of the classical method is to improve the accuracy of the boundary-derivative calculations. To give some idea as to the accuracy of the approximate solutions in the entire range, some results are presented in Figs. 2-4. It is clear from these figures that present solutions have practically the same degree of accuracy as the classical integral solutions, although the new idea of calculating boundary derivatives gives substantially improved accuracy in the boundary-derivative results. Table 1 summarizes the results of this model problem.

Table 1. Summary of Results of Model Problem

$$\frac{d^2y}{dx^2} = y;\ y(0) = 0,\ y(1) = 1$$

Calculation Method	$f = f_1 = Ax + (1-A)x^2$			$f = f_2 = Ax^2 + (1-A)x^3$		
	y'(0)	y'(1)	A	y'(0)	y'(1)	A
x-moment y'(1) = f'(1)	0.8589 (+0.9%)	1.3077 (-0.4%)	0.6923	0.8929 (+4.9%)	1.2857 (-2.1%)	1.7143
x-moment y'(0) = f'(0)	0.8462 (-0.6%)	1.3205 (+0.6%)	0.8462	Not Applicable (f'(0) = 0)		
y_d-moment y'(1) = f'(1)	0.8703 (+2.3%)	1.3174 (+0.3%)	0.6826	1.0465 (+23.0%)	1.4275 (+8.7%)	1.5725
y_i-moment y'(1) = f'(1)	0.8648 (+1.6%)	1.3127 (-0.02%)	0.6873	0.9139 (+7.4%)	1.3051 (-0.6%)	1.6949
x-mom. + y_d-mom.	0.8523 (+0.2%)	1.3144 (+0.1%)	0.7727	No Solution		
x-mom. + y_i-mom.	0.8537 (+0.3%)	1.3130 (0%)	0.7559	0.8769 (+3.1%)	1.3097 (-0.3%)	2.1930
Classical Integral	0.7692 (-9.6%)	1.2308 (-6.3%)	0.7692	0 (-100%)	0.4615 (-64.9%)	2.5385

EXACT Solution: $y = \frac{\sinh x}{\sinh 1}$; $y'(0) = 0.8509$, $y'(1) = 1.3130$

Percentage error = $\frac{(\text{APPRO.}) - (\text{EXACT})}{(\text{EXACT})}$ (indicated in parentheses)

In the following, the method is applied to some simple three-dimensional boundary-layer flow problems. For such problems, the boundary conditions are similar to the model problem just studied, except that only one boundary derivative i.e., the derivative at the wall, is of interest. The boundary derivative of any flow variables at the edge of the boundary layer is taken to be zero because of the boundary-layer flow is supposed to join smoothly to the other inviscid flow at the edge. For this reason, the more complicated version of the combined scheme is not used in most cases. However, it is used in one example in an effort to cope with the difficulty of homogeneous boundary conditions which require two parameters in the assumed profiles.

3. APPLICATION TO THREE-DIMENSIONAL BOUNDARY-LAYER FLOWS

Application of the present method to the solution of two-dimensional boundary-layer flows and one-dimensional transient heat conduction problems was reported in various previous publications, e.g., Refs. 1-4. For general three-dimensional boundary-layers, the present method will still lead to a coupled set of nonlinear partial differential equations whose solution would require numerical computations. As a first step to determine the feasibility of such applications, we are interested in obtaining only simple solutions without the expenditure of extensive numerical effort. Therefore, some relatively simple three-dimensional flows are studied in the following for which closed-form solutions can be obtained by the present method.

3.1 PARABOLIC INVISCID STREAMLINES ON A FLAT PLATE. Consider the boundary-layer flow past a semi-infinite flat plate with an infinite span (z dimension extends to $\pm\infty$). Suppose that the inviscid velocity on the plate has the components u_0 and bx in x and z directions, respectively. The inviscid surface streamlines are given by the equation

$$\frac{dz}{dx} = \frac{bx}{u_0} \tag{3.1}$$

from which the streamline equation is obtained as

$$z = z_0 + \frac{1}{2}\frac{b}{u_0}x^2 \tag{3.2}$$

Euler's equation then determines the pressure field as

$$-\frac{1}{\rho}\frac{dp}{dz} = u_0 b \tag{3.3a}$$

and

$$\frac{\partial p}{\partial x} = 0 \tag{3.3b}$$

This problem was first solved by Loos[6] who obtained the exact solution in similarity form.

The laminar boundary-layer equations in the rectangular cartesian coordinate system (x,y,z) are

6. Loos, H. G., "A Simple Laminar Boundary Layer with Secondary Flow," Journal of the Aeronautical Sciences, Vol. 22, 1955, pp. 35-40.

$$\frac{\partial u}{\partial x} + \frac{\partial v}{\partial y} = 0 \tag{3.4a}$$

$$u \frac{\partial u}{\partial x} + v \frac{\partial u}{\partial y} = \nu \frac{\partial^2 u}{\partial y^2} \tag{3.4b}$$

$$u \frac{\partial w}{\partial x} + v \frac{\partial w}{\partial y} = bu_0 + \nu \frac{\partial^2 w}{\partial y^2} . \tag{3.4c}$$

The boundary conditions are

$$y = 0: \quad u = v = w = 0 \tag{3.5a}$$

$$y \to \infty: \quad u \to u_0, \; w \to w_1 = bx \tag{3.5b}$$

$$x = 0: \quad u = u_0, \; w = bx \tag{3.5c}$$

Note that $\frac{\partial}{\partial z} \equiv 0$ because of the infinite extent of the flow field in z-direction. Eqs. (3.4a,b) represent the well-known Blasius flow which has been solved approximately by the present integral method in Ref. 1. The approximate solutions will be used in the solution of the spanwise flow, w.

3.1.1 Present Method. The present procedure of solving the spanwise flow is as follows. First, the spanwise momentum equation, Eq. (3.4c), is integrated across the spanwise boundary-layer thickness, δ_z, resulting in the spanwise momentum balance integral,

$$\frac{\tau_{wz}}{\rho} = \left(\frac{dw_1}{dx}\right) \int_0^{\delta_z} (u_0 - u)dy + \frac{d}{dx} \int_0^{\delta_z} u(w_1 - w)dy \tag{3.6}$$

where τ_{wz} is the spanwise skin friction.

Eq. (3.6) is to be used in conjunction with either the y-moment integral of Eq. (3.4c),

$$\int_0^{\delta_z} \frac{\partial}{\partial x} yuwdy + \int_0^{\delta_z} y \frac{\partial}{\partial y} uwdy = \frac{1}{2} bu_0 \delta_z^2$$

$$+ \nu \int_0^{\delta_z} y \frac{\partial^2}{\partial y^2} w \, dy \tag{3.7a}$$

or the w-moment integral of Eq. (3.4c),

$$\int_0^{\delta_z} w \frac{\partial}{\partial x} uwdy + \int_0^{\delta_z} w \frac{\partial}{\partial y} uwdy = bu_0 \int_0^{\delta_z} wdy$$

$$+ \nu \int_0^{\delta_z} w \frac{\partial^2}{\partial y^2} w \, dy \qquad (3.7b)$$

The use of Eq. (3.7a) corresponds to the y-moment scheme whereas the use of Eq. (3.7b) is referred to as the w-moment scheme.

The y-moment scheme will be used first. We assume the following simple (linear) profiles for u and w:

$$u/u_0 = \eta_x \; ; \quad \eta_x = y/\delta_x \qquad (3.8a)$$

$$w/bx = \eta_z \; ; \quad \eta_z = y/\delta_z \qquad (3.8b)$$

where δ_x is the chordwise boundary-layer thickness.

The chordwise-flow solution by the present method has been given in Ref. 1 as

$$\frac{R_{\delta x}}{R_x} = \frac{\delta_x}{x} = \frac{4}{\sqrt{R_x}} \qquad (3.9a)$$

and

$$\frac{1}{2} C_f \sqrt{R_x} = \frac{1}{3} \qquad (3.9b)$$

where $R_{\delta x} = \frac{u_0 \delta_x}{\nu}$, $R_x = \frac{u_0 x}{\nu}$ and $\frac{1}{2} C_f \equiv \tau_{wx}/\rho u_0^2$.

Substituting Eqs. (3.8a) and (3.8b) into Eq. (3.7a) and assuming that

$$\Delta \equiv \delta_z/\delta_x < 1 \qquad (3.10)$$

we obtain an ordinary differential equation:

$$\frac{1}{4} \frac{d}{dx} (\delta_z^2 \Delta x) - \frac{3}{8} \delta_z x \frac{d}{dx} (\Delta \delta_z)$$

$$- \frac{1}{4} x \delta_z \Delta \frac{d}{dx} z = \frac{1}{2} \delta_z^2 - \frac{\nu x}{u_0} \qquad (3.11)$$

Eq. (3.11) admits the simple solution of Δ = const, with Δ determined from the algebraic equation

$$3\Delta^3 - 8\Delta^2 + 1 = 0 \qquad (3.12)$$

The only self-consistent solution of Δ is

$$\Delta = 0.382, \tag{3.13}$$

The other two solutions, $\Delta = 2.618, -1/3$ are discarded.

The corresponding solution for the spanwise skin friction is

$$\frac{1}{2} C_{fz} \sqrt{R_x} \equiv \frac{\tau_{wz}}{\rho u_0 w_1} \sqrt{R_x} = 1.382 , \tag{3.14}$$

compared to the exact solution[6] of $\frac{1}{2} C_{fz} \sqrt{R_x} = 1.414$.

The problem is next solved using the w-moment scheme. Two spanwise velocity profiles

$$\frac{w}{bx} = f_1 = \eta_z , \tag{3.15a}$$

$$\frac{w}{bx} = f_4 = 2\eta_z - 2\eta_z^3 + \eta_z^4 \tag{3.15b}$$

are used in the calculation to determine the sensitivity of results to the profiles chosen. The chordwise flow is still solved approximately by the present method, using the linear profile, Eq. (3.8a). *It is noted here that the approximate* solution for the chordwise flow using the u-moment scheme is the same as that using the y-moment scheme.

The w-moment integral has the following form:

$$\frac{d}{dx} \int_0^{\delta_z} uw^2 dy - (bx)^2 \frac{d}{dx} \int_0^{\delta_z} u dy = 2bu_0 \int_0^{\delta_z} w dy - 2\nu \int_0^{\delta_z} \left(\frac{\partial w}{\partial y}\right)^2 dy \tag{3.16}$$

The last term on the right-hand side of Eq. (3.16) *can be evaluated by two* different approximations, leading to the so called w_d-moment scheme and w_i-moment scheme, respectively, discussed in §2.3.2. In the w_i-moment scheme,

$$\frac{\partial w}{\partial y} = \frac{1}{\nu} \left\{ bu_0(\delta_z - y) - w \frac{\partial}{\partial x} \int_0^y u dy + bx \frac{d}{dx} \int_0^{\delta_z} u dy - \frac{\partial}{\partial x} \int_y^{\delta_z} uw dy \right\} \tag{3.17}$$

The calculation based on w_i-moment scheme is obviously much more complicated, and is not included in the present report. Only w_d-moment scheme is used in the following calculation.

For $w = bxf_1$ and $u = u_0 x$, Eq. (3.16) reduces to

$$R_x \frac{d\Delta^2}{dR_x} - \frac{3}{2} \Delta^2 = -4\Delta + \frac{1}{2\Delta} \tag{3.18}$$

for $\Delta < 1$.

Eq. (3.18) again admits the solution Δ = const., and the equation for Δ is

$$3\Delta^3 - 8\Delta^2 + 1 = 0 \tag{3.19}$$

which is identical to the equation for the y-moment scheme, Eq. (3.12).

The solution is thus the same as that of the y-moment scheme,

$$\Delta = 0.382 \tag{3.20a}$$

$$\frac{1}{2} C_{fz} \sqrt{\bar{R}_x} = 1.382 \tag{3.20b}$$

For $w = bxf_4$ and $u = u_0 \eta_x$, Eq. (3.16) reduces to

$$2.9365\Delta^3 - 5.6\Delta^2 + 0.7429 = 0 \tag{3.20}$$

after assuming Δ = const. < 1. The self-consistent solution is determined to be

$$\Delta = 0.411? \tag{3.21}$$

where the other two solutions, Δ = 1.832, -0.336, are discarded.

The spanwise skin-friction coefficient is obtained from Eq. (3.6),

$$\frac{1}{2} C_{fz} \sqrt{\bar{R}_x} = 1.374. \tag{3.22}$$

3.1.2 Karman-Pohlhausen Method. The solution with the classical Karman-Pohlhausen (K-P) integral method makes use of the momentum integral, Eq. (3.6) alone, with τ_{wz} given by

$$\tau_{wz} = \mu bx \left(\frac{\partial f}{\partial y}\right)_0 .$$

Of course, the chordwise-momentum equation needs to be solved first. Here, the K-P solution based on the linear profile is taken from Ref. 1, i.e.,

$$R_\delta = 2\sqrt{3} \sqrt{\bar{R}_x} \tag{3.23a}$$

and

$$\frac{1}{2} C_f \sqrt{\bar{R}_x} = 0.2887 \tag{3.23b}$$

For the linear spanwise velocity profile, Eq. (3.15a), the quantity Δ is determined by the equation

$$3\Delta^3 - 12\Delta^2 + 1 = 0 \tag{3.24}$$

The self-consistent solution is

$$\Delta = 0.3 \ , \tag{3.25}$$

and the other two solutions, $\Delta = 3.979; -0.279$ are rejected.

The corresponding solution for skin friction is

$$C_{fz}\sqrt{R_x} = 0.962 \tag{3.26}$$

For $f = f_4$ (Eq. 3.15b), the equation for Δ is

$$2.4\Delta^3 - 6\Delta^2 + 1 = 0 \tag{3.27}$$

and the self-consistent solution is

$$\Delta = 0.4509 \tag{3.28}$$

The other solutions, $\Delta = 2.915, -0.3802$, are discarded.

Corresponding to this solution, we have

$$C_{fz}\sqrt{R_x} = 1.2804 \tag{3.29}$$

These K-P solutions are obviously inadequate in accuracy.

Results of this example are summarized in Table 2. It is clear that the present solutions are considerably better than the classical integral solution both in accuracy and in profile-sensitivity.

Table 2. Spanwise Skin-Friction Results for Parabolic Streamlines

W PROFILE	PRESENT METHOD		CLASSICAL K-P	
$(u = u_0\, y/\delta_x)$	$1/2C_{fz}R_x^{1/2}$	ERROR	$1/2C_{fz}R_x^{1/2}$	ERROR
$\frac{w}{w_1} = y/\delta_z$	1.382(w-mom.) 1.382(y-mom.)	-2.3%	0.962	-32.0%
$\frac{w}{w_1} = 2(y/\delta_z)$ $-2(y/\delta_z)^3+(y/\delta_z)^4$	1.374(w-mom.)	-2.82%	1.280	-9.5%

3.2 INFINITE SWEPTBACK WINGS. We next consider the laminar boundary-layer on an infinite sweptback wing (Fig. 5). Only the special case where the inviscid chordwise velocity varies as a power of x, i.e., $u_1 = cx^m$ and the inviscid spanwise velocity is a constant, i.e., $w_1 = w_\infty$, is solved. Exact solutions and classical K-P solutions of the problem can be found in Cooke[7].

Again, the chordwise flow is independent of the spanwise flow and can be solved separately. The exact solution (Falkner-Skan flow) is available in Smith[8].

The y-moment scheme is used here to give the approximate solution for the chordwise flow. A fourth degree polynomial profile

$$\frac{u}{u_1} = 2\eta_x - 2\eta_x^3 + \eta_x^4 + \frac{\lambda}{6}\eta_x(1-\eta_x)^3 \tag{3.30}$$

is used in the calculation, where

$$\lambda = \frac{\delta_x^2}{\nu}\frac{du_1}{dx} . \tag{3.31}$$

Note that $\lambda = \lambda(m)$ for $u_1 = cx^m$.

The y-moment integral reduces to the following algebraic equation:

$$-\frac{m}{m-1} = \frac{1}{\lambda}\frac{K(\lambda)}{\tilde{\alpha}(\lambda)} \tag{3.32a}$$

where

$$k(\lambda) = 2(1 - 0.1677\lambda + 0.005172\lambda^2 + 0.00010085\lambda^3) \tag{3.32b}$$

$$\tilde{\alpha}(\lambda) = 0.06135 - 0.001336\lambda - 0.00006779\lambda^2 \tag{3.32c}$$

The chordwise momentum balance integral gives the skin friction coefficient as

$$\frac{1}{2}C_{fx}\sqrt{R_x} = \frac{\tau_{wx}}{\frac{\rho}{2}u_1}\sqrt{\frac{u_e x}{\nu}} = \sqrt{\frac{m}{\lambda}}\left(2\tilde{\gamma} - \frac{1}{2}\frac{m-1}{m}\tilde{\gamma} + \tilde{\beta}\right)\lambda \tag{3.33a}$$

7. Cooke, J. C., "Pohlhausen's Method for Three-Dimensional Laminar Boundary Layers," Aeronautical Quarterly, Vol. 3, 1951, pp. 51-60.
8. Smith, A. M. O., "Rapid Laminar Boundary-Layer Calculations by Piecewise Application of Similar Solutions," Journal of the Aeronautical Sciences, Vol. 23, No. 10, Oct 1956, pp. 901-912.

where

$$\tilde{\gamma} = 0.11746 - 0.0010582\lambda - 0.00011023\lambda^2 \tag{3.33b}$$

and

$$\tilde{\beta} = 0.3 - 0.0083333\lambda \tag{3.33c}$$

Eqs. (3.32) and (3.33) combine to give the solution of

$$\frac{1}{2} C_{fx} \sqrt{R_x}$$

as a function of m. The results are shown in Figs. 6 and 7 for $\beta > 0$ and $\beta < 0$, respectively. ($\beta = 2m/m+1$ = pressure gradient parameter). Exact solutions and classical K-P solutions are also included for comparison. As expected, the classical integral solution for the accelerating flows ($\beta > 0$) is very accurate, and the improvement by the present method is rather insignificant especially for large β. In the case of adverse pressure gradient, however, the present method appears to offer substantial improvements except near separation ($\beta = -0.1988$).

The spanwise boundary layer is then studied. A polynomial profile

$$\frac{w}{w_\infty} = 2\eta_z - 2\eta_z^3 + \eta_z^4 \tag{3.34}$$

is assumed, and the y-moment integral of the spanwise momentum equation reduces to the following algebraic equation for $\Delta(= \delta_z/\delta_x)$

$$\Delta^3\lambda\left[\frac{1}{14}\left(1 + \frac{\lambda}{12}\right) - \frac{\lambda\Delta}{140} + \frac{1}{72}\left(-1 + \frac{\lambda}{4}\right)\Delta^2 + \frac{2}{525}\left(1 - \frac{\lambda}{6}\right)\Delta^3\right] = \beta \tag{3.35}$$

Eq. (3.35) is derived on the assumption of $\Delta < 1$ which corresponds to the case of adverse pressure gradient, $\beta < 0$. This is the case for which an improvement on the older integral solution is most desired.

The spanwise momentum balance integral yields an expression for the spanwise skin friction

$$\frac{1}{2} C_{fz} \sqrt{R_x} = \frac{\tau_{wz}}{\rho u_1 w_\infty} \sqrt{\frac{u_1 x}{\nu}} = \Delta^2 \frac{\lambda}{\beta} \sqrt{\frac{m}{\lambda}}\, k_1(\lambda,\Delta) \tag{3.36a}$$

where

$$k_1(\lambda,\Delta) = \frac{1}{15}\left(2 + \frac{\lambda}{6}\right) - \frac{1}{84}\lambda\Delta + \frac{3}{140}\left(-1 + \frac{\lambda}{4}\right)\Delta^2 + \frac{1}{180}\left(1 - \frac{1}{6}\lambda\right)\Delta^3 \tag{3.36b}$$

Eqs. (3.32), (3.35) and (3.36) then give the solution of

$$\frac{1}{2} C_{fz} \sqrt{R_x}$$

as a function of the pressure gradient parameter, $\beta(= 2m/(m+1))$. The results are shown in Fig. 8, along with exact solutions and older integral solutions[7]. The present solutions only show a modest improvement on the classical integral solutions for moderately adverse pressure gradients in this class of flow.

3.3 CIRCULAR INVISCID STREAMLINES ON A FLAT PLATE.

3.3.1 Formulation Using Inviscid Streamline Coordinates. Consider the boundary-layer flow on a semi-infinite flat plate with circular inviscid streamlines (Fig. 9). We use the inviscid streamline as one of the coordinate axis so that the cross flow, w, caused by the centrifugal force would vanish at both ends of the spanwise boundary layer. Only the case of small total turning angle, β, is considered, so that the cross-flow velocity is an order of magnitude smaller than the main flow velocity. This problem was studied earlier by Mager and Hansen[9], and the exact solution is available in Ref. 9. The boundary-layer equations in the streamline coordinate system for small turning angle, $(cx)^2 << 1$, are given below:

$$\frac{\partial}{\partial x} u + \frac{\partial}{\partial y} (1 + cz)v = 0 \tag{3.37a}$$

$$\frac{u}{1+cz} \frac{\partial u}{\partial x} + v \frac{\partial u}{\partial y} = \nu \frac{\partial^2 u}{\partial y^2} \tag{3.37b}$$

$$\frac{u}{1+cz} \frac{\partial w}{\partial x} + v \frac{\partial w}{\partial y} = - \frac{c}{1+cz} (u_1^2 - u^2) + \nu \frac{\partial^2 w}{\partial y^2} \tag{3.37c}$$

The boundary conditions are:

$$y = 0: \quad u = v = w = 0 \tag{3.38a}$$

$$y \to \infty: \quad u \to u_1(z), \; w \to 0 \tag{3.38b}$$

$$x = 0: \quad u = u_1(z), \; w = 0 \tag{3.38c}$$

Note that the cross flow, w, has homogeneous boundary conditions in this formulation.

The new variables

$$\tilde{v} = (1+cz)^{1/2} v, \quad \tilde{y} = (1+cz)^{-1/2} y \tag{3.39}$$

are then used to reduce Eqs. (3.37) to the following form:

9. Mager, A. and Hansen, A. G., "Laminar Boundary Layer Over Flat Plate in a Flow Having Circular Streamlines," NACA TN 2658, Mar 1952.

$$\frac{\partial u}{\partial x} + \frac{\partial \tilde{v}}{\partial \tilde{y}} = 0 \tag{3.40a}$$

$$u \frac{\partial u}{\partial x} + \tilde{v} \frac{\partial u}{\partial \tilde{y}} = \nu \frac{\partial^2 u}{\partial \tilde{y}^2} \tag{3.40b}$$

$$u \frac{\partial w}{\partial x} + \tilde{v} \frac{\partial w}{\partial \tilde{y}} = - c(u_1^2 - u^2) + \nu \frac{\partial^2 w}{\partial \tilde{y}^2} \tag{3.40c}$$

Obviously, Eqs. (3.40a) and (3.40b) correspond to the Blasius flow in the $(x,\tilde{y})$ plane, and the approximate solution by the present method has been obtained earlier[1], i.e., for

$$u/u_1 = \eta_x \equiv y/\delta_x, \quad \frac{1}{2} C_{fx} \sqrt{1+cz}\, \sqrt{R_x} = \frac{1}{3} .$$

This solution will be used in the cross-flow calculations.

The cross-flow moment balance integral is first obtained by integrating Eq. (3.40c) across the cross-flow boundary layer, i.e.,

$$\nu \left(\frac{\partial w}{\partial \tilde{y}}\right)_w = - \int_0^{\tilde{\delta}_z} c(u_1^2 - u^2) d\tilde{y} - \frac{d}{dx} \int_0^{\tilde{\delta}_z} uw d\tilde{y} \tag{3.41a}$$

where the boundary conditions of vanishing w at $\tilde{y} = 0, \tilde{\delta}_z$ have been used.

In dimensionless form, Eq. (3.41a) can be written as

$$\frac{1}{2} C_{fz} \sqrt{1+cz} = -c\tilde{\delta}_z \int_0^1 \left(1 - \frac{u^2}{u_1^2}\right) d\eta_z - \frac{d}{dx} \int_0^1 \tilde{\delta}_z \frac{u}{u_1} \frac{w}{u_1} d\eta_z \tag{3.41b}$$

where $\frac{1}{2} C_{fz} \equiv \frac{\tau_{wz}}{\rho u_1^2}$.

The y-moment integral of the cross-flow equation reduces to

$$\frac{d}{dx} \int_0^{\tilde{\delta}_z} \tilde{y} \frac{u}{u_1} \frac{w}{u_1} d\tilde{y} + \int_0^{\tilde{\delta}_z} \frac{w}{u_1} d\tilde{y} \frac{\partial}{\partial x} \int_0^{\tilde{y}} \frac{u}{u_1} d\tilde{y} - c \int_0^{\tilde{\delta}_z} \tilde{y} \left(\frac{u}{u_1}\right)^2 d\tilde{y} = - \frac{c\tilde{\delta}_z^2}{2} , \tag{3.41}$$

and the w-moment integral of the cross-flow equation is

$$\frac{d}{dx} \int_0^{\tilde{\delta}_z} \frac{u}{u_1} \left(\frac{w}{u_1}\right)^2 d\tilde{y} = -2c \int_0^{\tilde{\delta}_z} \frac{w}{u_1} d\tilde{y} + 2c \int_0^{\tilde{\delta}_z} \left(\frac{u}{u_1}\right)^2 \frac{w}{w_1} d\tilde{y} - \frac{2\nu}{u_1^3} \int_0^{\tilde{\delta}_z} \left(\frac{\partial w}{\partial \tilde{y}}\right)^2 d\tilde{y} \tag{3.42}$$

where $\tilde{y} = \tilde{\delta}_z$ represents the edge of the cross-flow boundary layer.

We assume the following profiles for use in the calculations, ($\eta_z \equiv \tilde{y}/\tilde{\delta}_z$, $\Delta \equiv \tilde{\delta}_z/\delta_x$);

$$\frac{u}{u_1} = f(\eta_x) = \eta_x = \Delta\eta_z, \tag{3.43a}$$

$$\frac{w}{u_1 cx} = g(\eta_z) = k\eta_z(\eta_z - 1) \tag{3.43b}$$

so that the boundary conditions of zero velocity at y = 0 and $\tilde{y} = \tilde{\delta}_z$ are satisfied. Also, we assume that $\Delta < 1$ so that Eq. (3.43a) can be used to represent u in the entire interval $0 \leq \tilde{y} \leq \tilde{\delta}_z$. The additional profile constant, k, in Eq. (3.43b) is the special feature peculiar to the problem with homogeneous boundary conditions (k = 1 is only a special profile in this family). Because of the additional constant, an additional equation is required to solve the problem. Therefore, in this formulation, the combined y-moment and w_d-moment scheme and the combined y-moment and zeroth-moment scheme will be used in the solution. The so-called zeroth-moment scheme is the same as the familiar K-P equation (i.e., momentum balance integral).

Consider the combined y-moment and w_d-moment scheme first. Substitution of Eqs. (3.43) into Eq. (3.41) and Eq. (3.42) leads, respectively, to the following equations:

$$\Delta^2 + \frac{7}{20} k\Delta - 2 = 0 \tag{3.44a}$$

and

$$128\Delta^4 + 5k\Delta^3 - 40\Delta^2 + 5k = 0 \tag{3.44b}$$

The solution of the above equations with Δ in the range of $0 \leq \Delta \leq 1$ is found to be

$$\Delta \approx 1, \; k = \frac{20}{7} \tag{3.45}$$

We note that the actual solution of Δ is slightly greater than 1, but $\Delta = 1$ is considered acceptable as a solution.

With Eqs. (3.43), Eq. (3.41b) yields the cross-flow skin friction result as

$$\frac{1}{2} c_{fz} \sqrt{1+cz} = - cx\Delta\left(4 - \frac{1}{2}k\Delta - \frac{4}{3}\Delta^2\right)/\sqrt{R_x} \tag{3.46}$$

which, upon substituting the solution, Eq. (3.45), gives

$$- \frac{1}{2} c_{fz} \sqrt{1+cz} \; \sqrt{R_x}/cx = 1.238 \tag{3.47}$$

The exact solution[9] gives

$$-\frac{1}{2} c_{fz} \sqrt{1+cz}\sqrt{\bar{R}_x}/cx = 1.082 \tag{3.48}$$

The accuracy of the present solution is not very satisfactory.

Next, we use the combined y-moment and zero-moment scheme. Here the same profiles, Eqs. (3.43) are used, but Eq. (3.41a) is used to replace Eq. (3.42). Eq. (3.41a) leads to the following algebraic equation:

$$k(1 + 2\Lambda^3) = 16\Lambda^2(1 - \tfrac{1}{3}\Lambda^2) \tag{3.49}$$

where $(\partial w/\partial \tilde{y})_w$ is taken to be $cxu_1(\partial g/\partial \tilde{y})_w$.

Eqs. (3.44a) and (3.49) give the following solution for Λ in the range $0 < \Lambda < 1$:

$$\Lambda = 0.891, \; k = 3.868 \tag{3.50}$$

and the skin friction follows from Eq. (3.41b):

$$-\frac{1}{2} c_{fz} \sqrt{1+cz}\sqrt{\bar{R}_x}/c_x = 1.0857 \tag{3.51}$$

The accuracy is seen to be remarkably good. We note that the same profile was also tried with the combined w_d-moment and zeroth-moment scheme, but no solution for Λ in the range $0 < \Lambda < 1$ exists.

Also, a different profile

$$g(\eta_z) = -k\eta_z(\eta_z-1)^2$$

has been tried with both the combined y-moment and w_d-moment scheme and the combined zeroth-moment and w_d-moment scheme. Again, no solution in the range $0 < \Lambda < 1$ can be obtained.

The above results indicate the disturbing difficulty of the present calculation procedure, namely, the strong dependence of the solution on the calculation schemes. Although the combined y-moment and zero-moment scheme gives almost exact solution for the cross-flow skin friction, the method itself when applied to this problem in its present formulation must be considered as somewhat unreliable in view of the unsatisfactory result with the combined y-moment and w_d-moment scheme. The difficulty is thought to be the homogeneous boundary conditions on w in the present streamline coordinate formulation. In the following, a different formulation will be used where the cross-flow velocity component is transformed into another variable which takes on a finite value at the edge of the boundary layer.

3.3.2 Modified Formulation. To avoid the aforementioned difficulty, we introduced a modified cross flow velocity, $\tilde{w}$, defined by

$$\tilde{w} = - w + cxu, \tag{3.52}$$

so that $\tilde{w}(\tilde{y} = 0) = 0$ and $\tilde{w}(\tilde{y} \to \infty) = cxu_1$.

Eq. (3.40c) is then transformed into the following form:

$$u \frac{\partial \tilde{w}}{\partial x} + \tilde{v} \frac{\partial \tilde{w}}{\partial \tilde{y}} = cu_1^2 + \nu \frac{\partial^2 w}{\partial \tilde{y}^2} \tag{3.53}$$

which resembles Eq. (3.4c) for the case of parabolic streamlines, as expected (see Ref. 6).

The present method is then successfully applied to solve for the modified cross-flow skin friction, $\tilde{C}_{fz}$. The original skin-friction coefficient, C_{fz}, is easily deduced from $\tilde{C}_{fz}$ by observing

$$\tilde{C}_{fz} = - C_{fz} + cx\, C_{fx} \tag{3.54}$$

where C_{fx} is assumed known (Ref. 1).

Now, define the modified cross-flow boundary-layer thickness $\tilde{\delta}_{1z}$ by requiring

$$\tilde{w}(\tilde{y} = \tilde{\delta}_{1z}) = cxu_1, \tag{3.55}$$

and assume that $\tilde{\delta}_{1z} < \tilde{\delta}$ where $u(\tilde{y} = \tilde{\delta}) = u_1$. Note that this definition of $\tilde{\delta}_{1z}$ would generally imply

$$w(\tilde{y} = \tilde{\delta}_{1z}) \neq 0. \tag{3.56}$$

Therefore, $\tilde{\delta}_{1z}$ is not the actual thickness of the cross-flow boundary layer.

Introducing dimensionless velocities

$$\tilde{w}^* \equiv \frac{\tilde{w}}{u_1}, \quad u^* \equiv \frac{u}{u_1}, \quad \tilde{v}^* \equiv \frac{\tilde{v}}{u_1} \tag{3.57}$$

we rewrite Eq. (3.53) as

$$\frac{\partial}{\partial x} u^* \tilde{w}^* + \frac{\partial}{\partial \tilde{y}} \tilde{v}^* \tilde{w}^* = c + \frac{\nu}{u_1} \frac{\partial^2 \tilde{w}^*}{\partial \tilde{y}^2} \tag{3.58}$$

Note that

$$\frac{\nu}{u_1} \frac{\partial \tilde{w}^*}{\partial \tilde{y}}\Big|_0 = \frac{\nu}{u_1^2} \left(- \frac{\partial w}{\partial y}\Big|_0 + cx \frac{\partial u}{\partial y}\Big|_0\right) \sqrt{1+cz} = \frac{1}{2}(- C_{fz} + cx\, C_{fx}) \sqrt{1+cz} \tag{3.59}$$

where, as before,

$$\frac{1}{2} C_{fz} \equiv \frac{\tau_{wz}}{\rho u_1^2}, \quad \frac{1}{2} C_{fx} \equiv \frac{\tau_{wx}}{\rho u_1^2} \tag{3.60}$$

Integrating Eq. (3.58) across the modified cross-flow boundary-layer thickness $\tilde{\delta}_{1z}$ leads to the expression for the modified cross-flow skin friction,

$$\frac{1}{2} \tilde{C}_{fz} \sqrt{1+cz} = c\tilde{\delta}_{1z} - \frac{d}{dx}\int_0^{\tilde{\delta}_{1z}} \tilde{u}^*\tilde{w}^* d\tilde{y} + cx \frac{d}{dx}\int_0^{\tilde{\delta}_{1z}} u^* d\tilde{y} \tag{3.61}$$

It is a straightforward procedure to apply the present method to the solution of the cross-flow equation. The cross-flow skin friction then follows from Eq. (3.61). Recall that the chordwise flow solution based on the linear profile

$$\frac{u}{u_1} = \tilde{y}/\tilde{\delta} = \Delta\tilde{y}/\tilde{\delta}_{1z} = \Delta\tilde{\eta}_{1z} \tag{3.62}$$

is given by

$$R_{\tilde{\delta}}^2 = 16R_x \tag{3.63a}$$

and

$$\frac{1}{2} C_{fx} \sqrt{R_x} = \frac{1}{3} \tag{3.63b}$$

where $R_{\tilde{\delta}} \equiv u_1\tilde{\delta}/\nu$ and $R_x \equiv u_1 x/\nu$.

The $\tilde{y}$-moment integral solution gives the following equation

$$28\Delta^3 \int_0^1 \tilde{\eta}_{1z} g(\tilde{\eta}_{1z}) d\tilde{\eta}_{1z} - 4\Delta^3 = 8\Delta^2 - 1 \tag{3.64}$$

where

$$g(\tilde{\eta}_{1z}) \equiv \tilde{w}^*/cx$$

is the modified cross-flow velocity profile.

(i) $g = \tilde{\eta}_{1z}$: $\Delta = 0.382$; $\frac{1}{2} \tilde{C}_{fz} \sqrt{1+cz}\sqrt{R_x}/cx = 4\Delta - \Delta^2 = 1.382$

(ii) $g = 2\tilde{\eta}_{1z} - 2\tilde{\eta}_{1z}^3 + \tilde{\eta}_{1z}^4$: $\Delta = 0.4045$; $\frac{1}{2} \tilde{C}_{fz} \sqrt{1+cz}\sqrt{R_x}/cx = 4\Delta - \frac{8}{5}\Delta^2 = 1.356$

(iii) $g = \frac{3}{2}\tilde{\eta}_{1z} - \frac{1}{2}\tilde{\eta}_{1z}^3$: $\Delta = 0.397$; $\frac{1}{2} \tilde{C}_{fz} \sqrt{1+cz}\sqrt{R_x}/cx = 4\Delta - \frac{7}{5}\Delta^2 = 1.367$

The results are summarized in Table 3. Note that different profiles for $\tilde{w}$ are employed to determine the sensitivity of results to profiles. The results for the w_d-moment scheme are taken directly from §3.1 (see Table 2).

Table 3. Cross-Flow Skin Friction, C_{fz}, for Circular Streamlines (Small Turning); $\frac{u}{u_1} = \tilde{\eta}$

$\tilde{w}/cxu_1$	Scheme	$\frac{1}{2}\tilde{C}_{fz}\sqrt{1+cz}\sqrt{R_x}/cx$	$-\frac{1}{2}C_{fz}\sqrt{1+cz}\sqrt{R_x}/cx$	Error
$\tilde{\eta}_{1z}$	$\tilde{w}_d$-moment	1.382	1.049	-3.0%
$2\tilde{\eta}_{1z}-2\tilde{\eta}_{1z}^3+\tilde{\eta}_{1z}^4$	$\tilde{w}_d$-moment	1.374	1.041	-3.8%
$\tilde{\eta}_{1z}$	$\tilde{y}$-moment	1.382	1.049	-3.0%
$2\tilde{\eta}_{1z}-2\tilde{\eta}_{1z}^3+\tilde{\eta}_{1z}^4$	$\tilde{y}$-moment	1.356	1.023	-5.5%
$\frac{3}{2}\tilde{\eta}_{1z}-\frac{1}{2}\tilde{\eta}_{1z}^3$	$\tilde{y}$-moment	1.367	1.034	-4.4%
EXACT			1.082	

$$\text{Error} = \frac{\text{(Approx.)} - \text{(Exact)}}{\text{(Exact)}}$$

It is obvious that the present method yields very satisfactory results to tne problem in the new formulation.

4. SUMMARY AND CONCLUDING REMARKS

The formulation of the new integral method is demonstrated in various schemes, and a model problem of ordinary differential equation is used as an example of application of these schemes. Extensive comparisons are made of the approximate solutions and the exact solution to determine the strengths and weaknesses of various calculation schemes. Emphasis is placed on the calculation of boundary derivatives which in physical applications are related to quantities of the greatest practical interest. While the results appear insufficient to yield a conclusive assessment of the relative merits, they do seem to indicate the superiority of the more complicated scheme of combined moments, i.e., use of two moment equations in addition to the integrated version of the original differential equation. Also, the study clearly demonstrates the importance of a qualitative understanding of the behavior of the exact solution in achieving good results. In all cases studied, the present solutions are all found to be substantially better than those of the classical integral method.

Preliminary results of application of the integral method developed by the author to three-dimensional boundary layers are also reported. Only simple flows are studied in this paper, and the results are presented in terms of the spanwise (or cross flow) skin friction. The results continue to be encouraging, although

in cases where the classical Karman-Pohlhausen method already proves to be adequate, the improvement over the classical integral solution does not seem to be significant.

These preliminary studies seem to suggest that the application of the present method to cross flows in the streamline coordinate system requires special care. The choice of a proper velocity profile which vanishes at both ends of the boundary layer requires careful consideration.

In the application to turbulent boundary layers, the momentum balance integral remains applicable if the mean velocity is used and if the normal components of the Reynolds stress are small, as they usually are. Therefore, the classical K-P method makes no distinction between turbulent flows and laminar flows. However, the moment equations that appear in the present method do require a knowledge of the turbulent stress distribution in the boundary layer when applied to turbulent flows. Therefore, the present integral method can be used with different turbulence models in the turbulent boundary layer calculations.

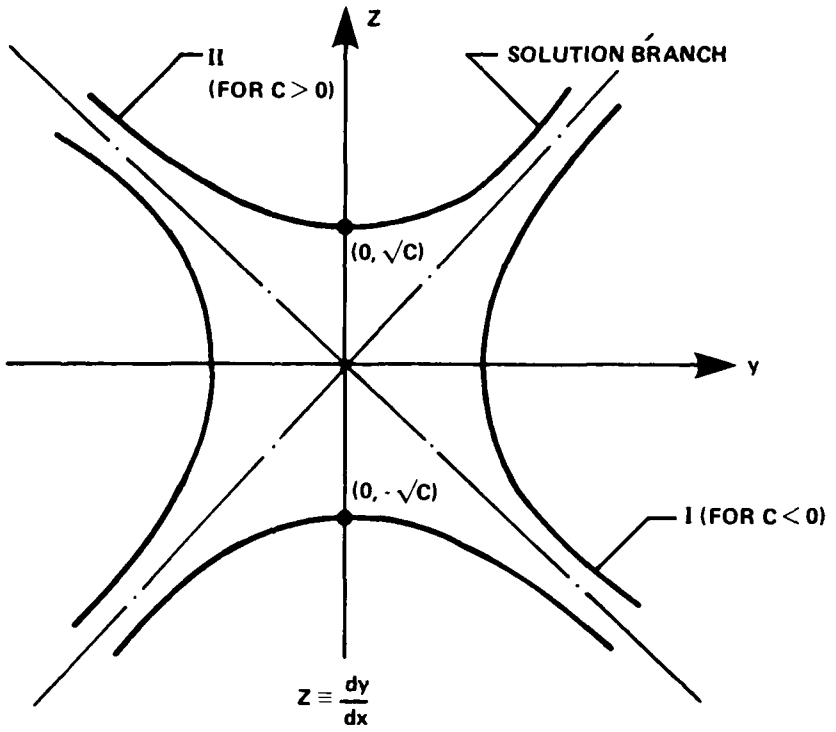

FIGURE 1 BEHAVIOR OF EXACT SOLUTION OF MODEL PROBLEM

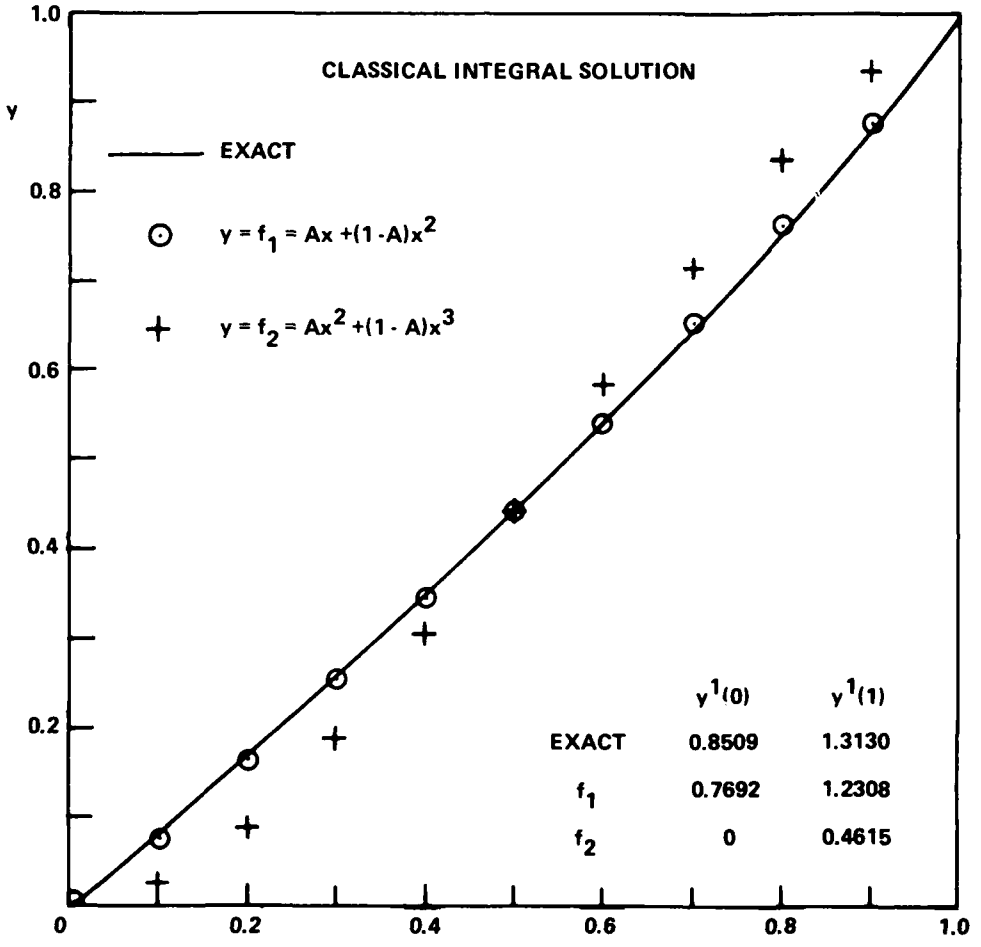

FIGURE 2 CLASSICAL INTEGRAL SOLUTION OF MODEL PROBLEM

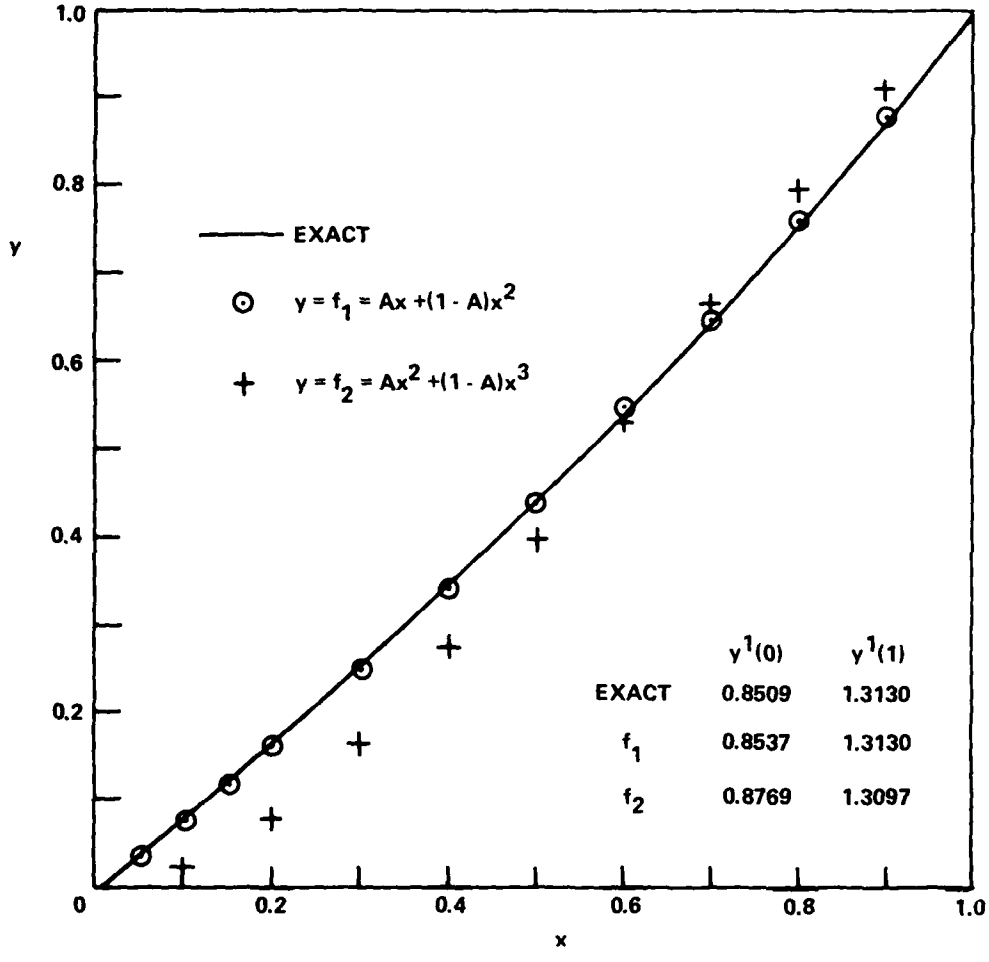

FIGURE 3 PRESENT INTEGRAL SOLUTION OF MODEL PROBLEM (COMBINED X-MOMENT AND Yi - MOMENT SCHEME)

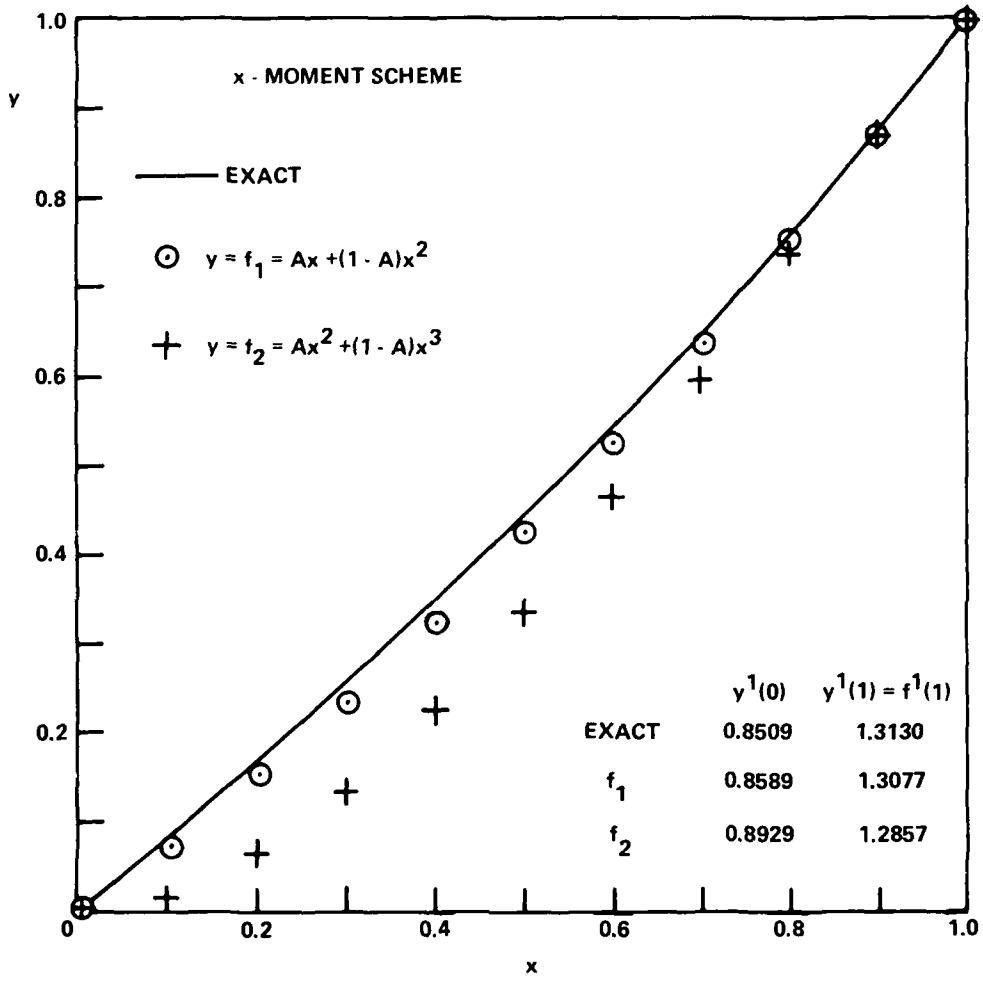

FIGURE 4 PRESENT INTEGRAL SOLUTION OF MODEL PROBLEM (X - MOMENT SCHEME)

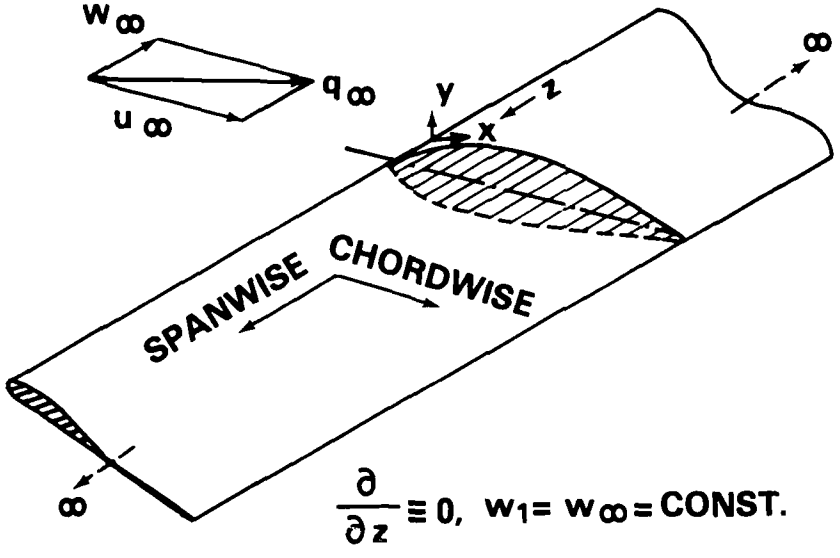

FIGURE 5 INFINITE SWEPT WING - GEOMETRY

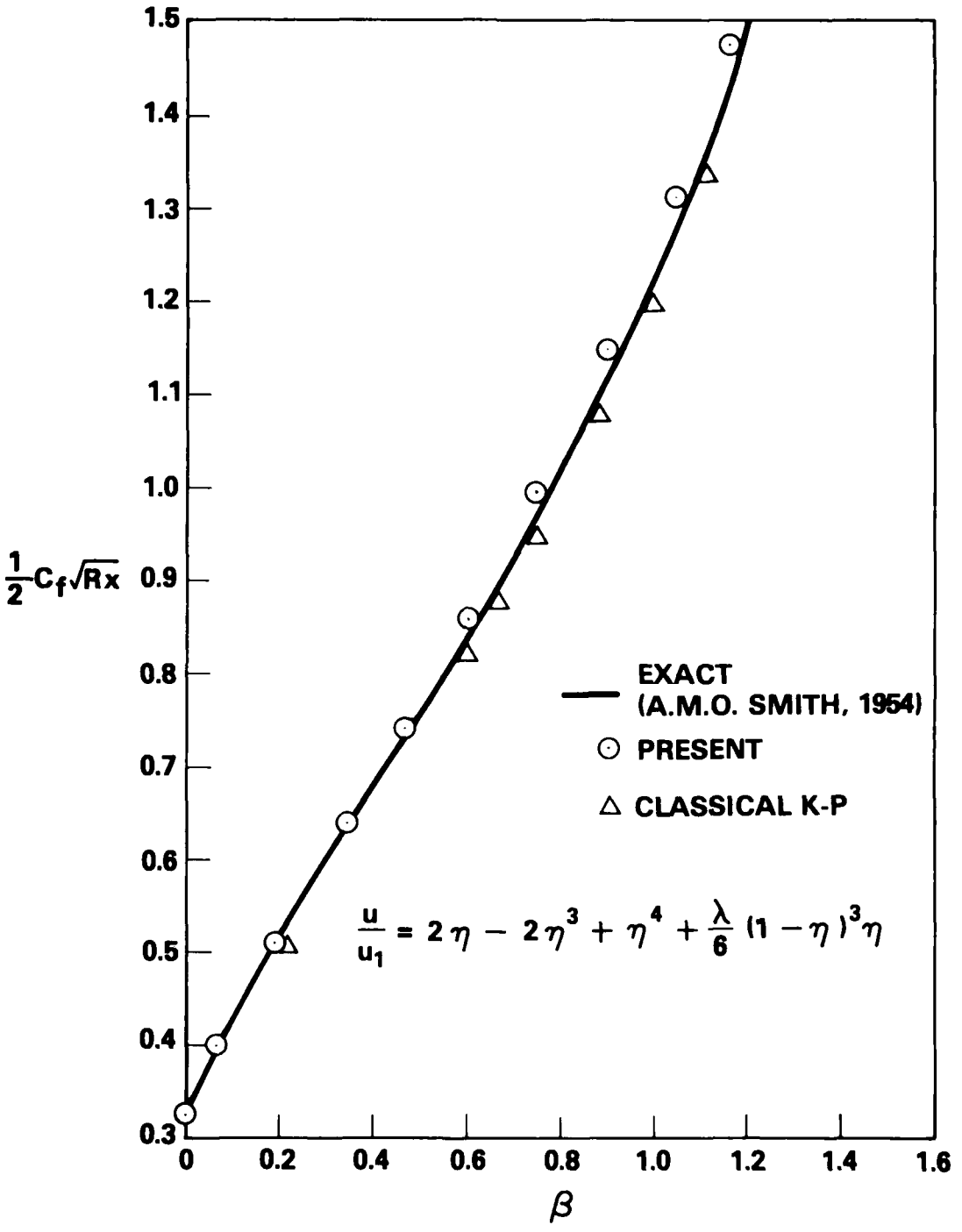

FIGURE 6 INFINITE SWEPT WEDGE - CHORDWISE SKIN FRICTION FOR $\beta > o$

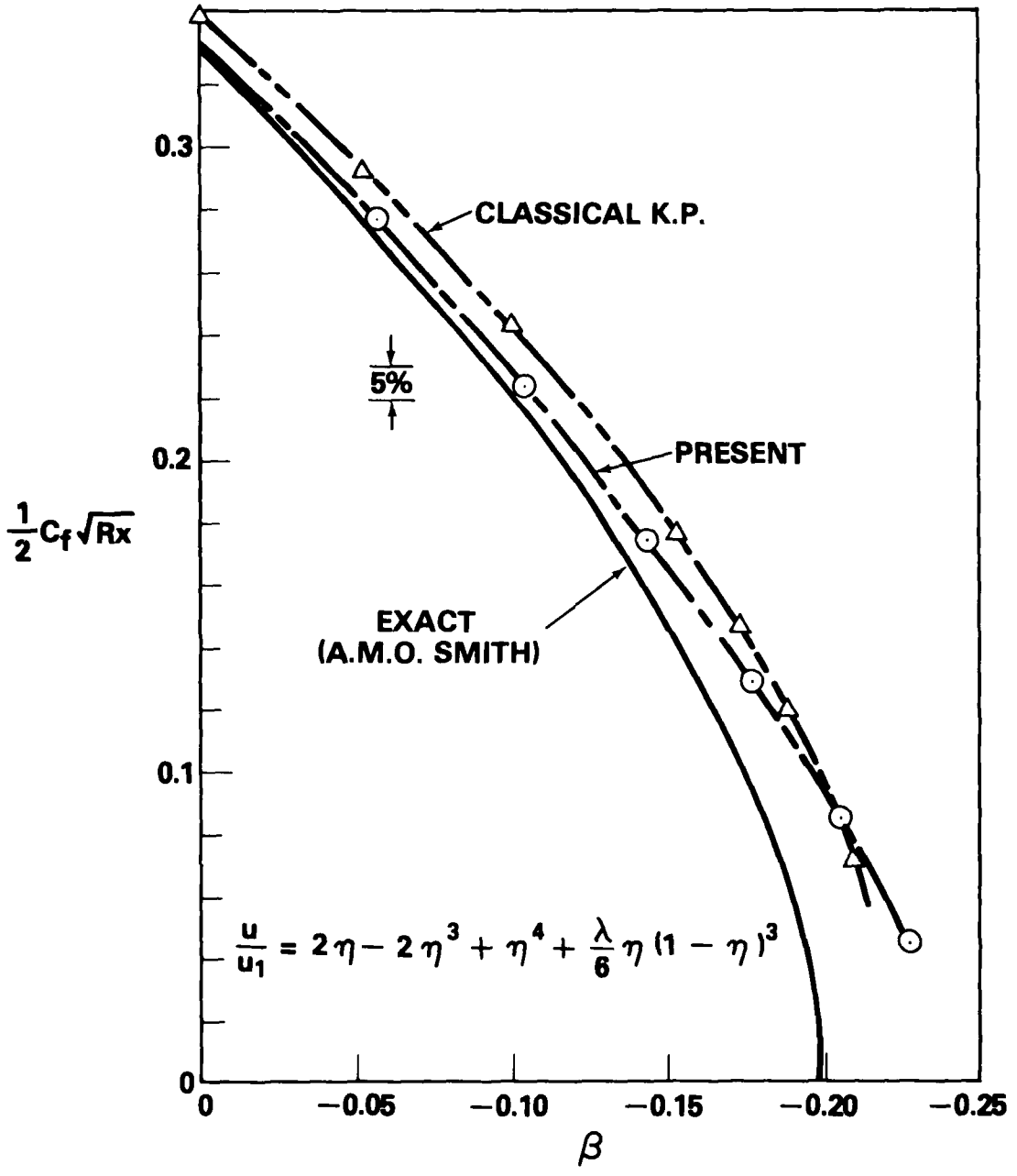

FIGURE 7 INFINITE SWEPT WEDGE - CHORDWISE SKIN FRICTION FOR $\beta < o$

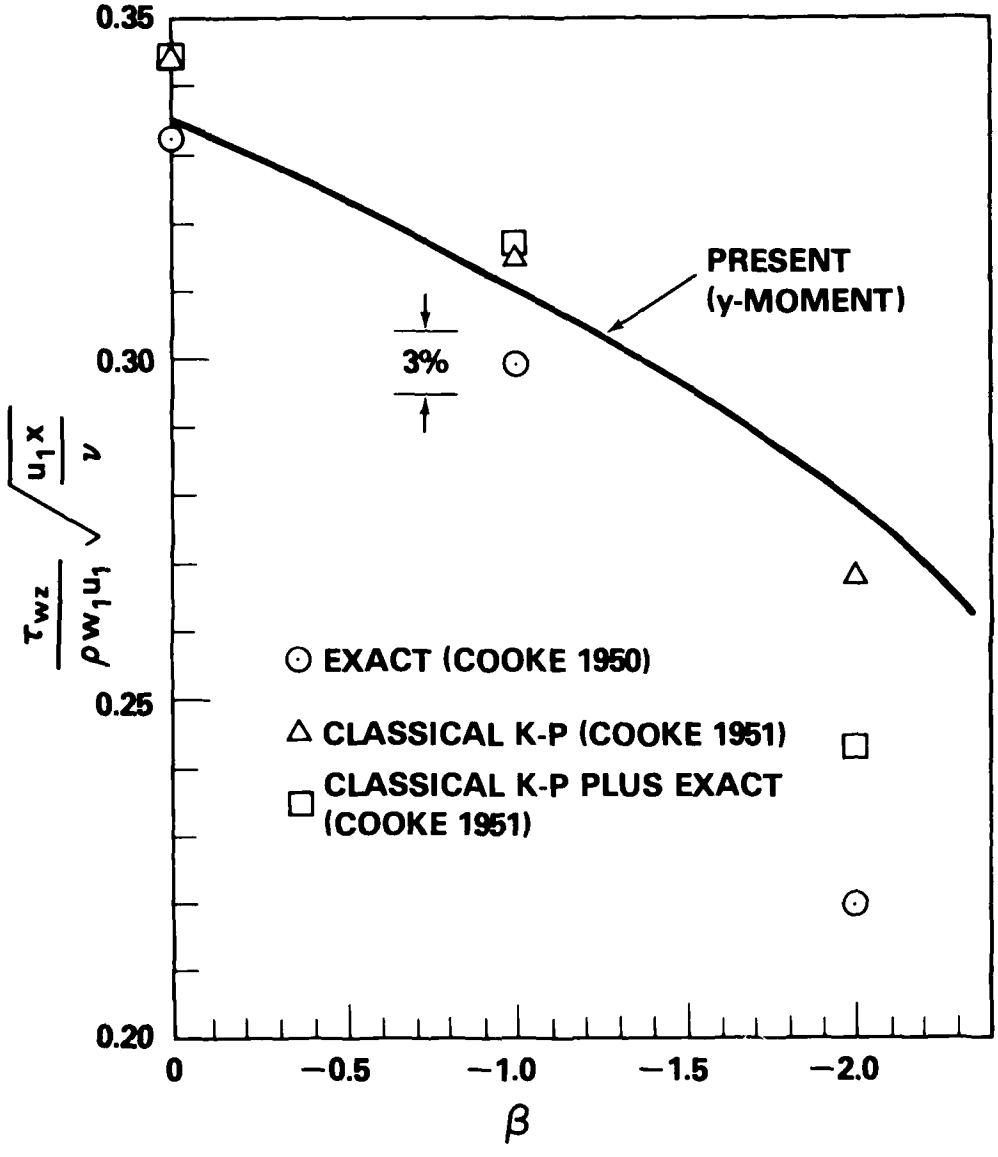

FIGURE 8 INFINITE SWEPT WEDGE - SPANWISE SKIN FRICTION

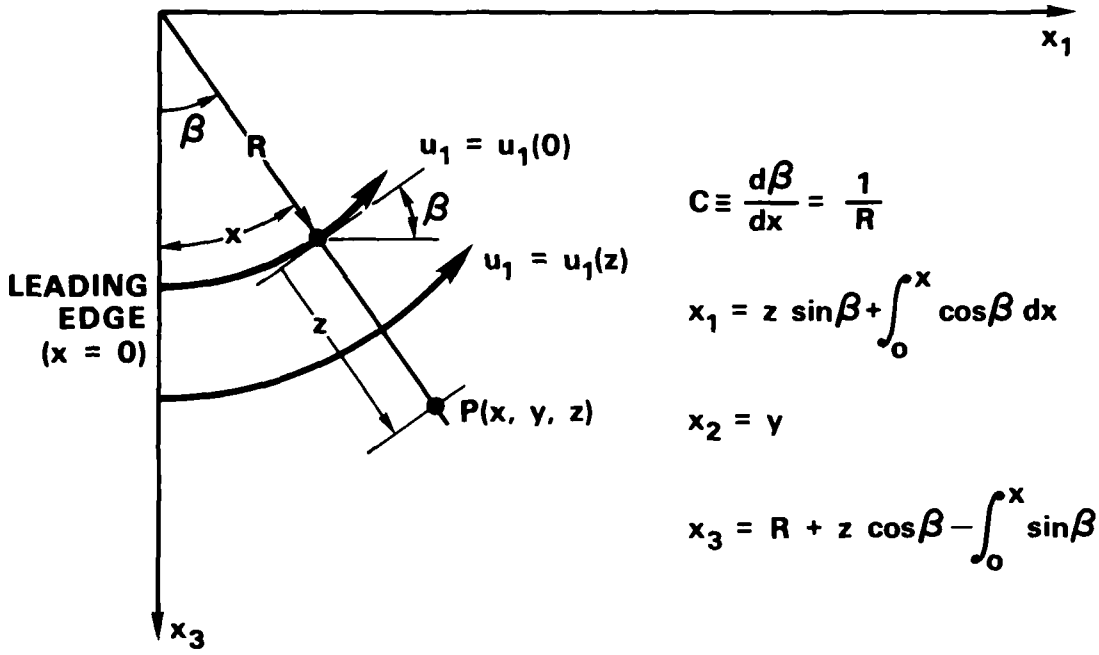

$$C \equiv \frac{d\beta}{dx} = \frac{1}{R}$$

$$x_1 = z \sin\beta + \int_0^x \cos\beta \, dx$$

$$x_2 = y$$

$$x_3 = R + z \cos\beta - \int_0^x \sin\beta \, dx$$

FIGURE 9 FLAT PLATE BOUNDARY LAYER WITH CIRCULAR STREAMLINES COORDINATE SYSTEM

REFERENCES

1. Zien, T. F., "A New Integral Calculation of Skin Friction on a Porous Plate," AIAA Journal, Vol. 9, No. 7, Jul 1971, pp. 1423-1425.

2. Zien, T. F., "Approximate Analysis of Heat Transfer in Transpired Boundary Layer with Effects of Prandtl Number," International Journal of Heat and Mass Transfer, Vol. 19, No. 5, May 1976, pp. 513-521.

3. Zien, T. F., "Study of Heat Conduction with Phase Transition Using an Integral Method," AIAA Progress in Astronautics and Aeronautics, Vol. 56, Thermophysics of Spacecraft and Outer Planet Entry Probes (Ed. A. M. Smith), Sep 1977, pp. 87-111.

4. Zien, T. F., "Integral Solutions of Ablation Problems with Time-Dependent Heat Flux," AIAA Journal, Vol. 16, No. 12, Dec 1978, pp. 1287-1295.

5. King, W. S., "An Approximate Method for Estimating the Critical Reynolds Number for a Heated Flat Plate in Water," Rand Paper Series P-6176, The Rand Corporation, Santa Monica, Calif., Aug 1978.

6. Loos, H. G., "A Simple Laminar Boundary Layer with Secondary Flow," Journal of the Aeronautical Sciences, Vol. 22, 1955, pp. 35-40.

7. Cooke, J. C., "Pohlhausen's Method for Three-Dimensional Laminar Boundary Layers," Aeronautical Quarterly, Vol. 3, 1951, pp. 51-60.

8. Smith, A. M. O., "Rapid Laminar Boundary-Layer Calculations by Piecewise Application of Similar Solutions," Journal of the Aeronautical Sciences, Vol. 23, No. 10, Oct 1956, pp. 901-912.

9. Mager, A. and Hansen, A. G., "Laminar Boundary Layer Over Flat Plate in a Flow Having Circular Streamlines," NACA TN 2658, Mar 1952.

DISTRIBUTION

Commander
Naval Sea Systems Command
Attn: SEA-05121 (Chief Technical Analyst)
SEA-033
SEA-03I
SEA-09G32 2
SEA-03B
Department of the Navy
Washington, DC 20362

Commander
Naval Air Systems Command
Attn: AIR-03B
AIR-03C
AIR-320
AIR-320C (William C. Volz)
AIR-310 (Dr. H. J. Mueller)
AIR-50174 2
Department of the Navy
Washington, DC 20361

Office of Naval Research
Attn: ONR-430B (Morton Cooper) 2
CDR R. D. Matulka
800 N. Quincy Street
Arlington, VA 22203

Commander
David W. Taylor Naval Ship Research and
Development Center
Attn: 5641 (Central Library Branch)
5643 (Aerodynamic Laboratory)
Dr. T. C. Tai
Dr. C. von Kerczek
Bethesda, MD 20034

Commander
Naval Weapons Center
Attn: 3161 (Bertha Ryan, W. R. Compton,
C. F. Markarian, Ray Van Aken)
533 (Technical Library)
406
4063 (R. E. Meeker)
China Lake, CA 93555

Director
Naval Research Laboratory
Attn: Library
6503
Washington, DC 20375

DISTRIBUTION (Cont.)

NASA
Langley Station
Attn: MS/185 (Technical Library)
Aero & Space Mech Div.
Dennis Bushwell
Ivan Beckwith
R. Trimpi
MS/164 (J. B. Anders)
Hampton, VA 23665

NASA
Lewis Research Center
Attn: 60-3 (Library)
Chief, Wind Tunnel and Flight Division
21000 Brookpart Road
Cleveland, OH 44135

NASA
George C. Marshall Space Flight Center
Attn: R-AERO-AU (T. Reed)
ED31 (W. K. Dahm)
Huntsville, AL 35812

NASA
Attn: RR (Dr. H. H. Kurzweg)
600 Independence Avenue S.W.
Washington, DC 20546

NASA
P. O. Box 33
College Park, MD 20740

Technical Library
Director Defense Research and
Engineering (DDR&E)
Attn: Stop 103
Room 3E-1063, The Pentagon
Washington, DC 20301

Defense Documentation Center
Cameron Station
Alexandria, VA 22314 12

Commander
Naval Missile Center
Attn: Technical Library
Point Mugu, CA 93041

DISTRIBUTION (Cont.)

Commanding Officer
USA Aberdeen Research and Development Center
Attn: STEAP-TL (Technical Library Division)
AMXRD-XSE
Aberdeen Proving Ground, MD 21005

Director
Strategic Systems Project Office
Attn: NSP-2722 2
Department of the Navy
Washington, DC 20390

Director of Intelligence
Attn: AFOIN-3B
Headquarters, USAF (AFNINDE)
Washington, DC 20330

Commander
Space and Missile Systems Organization
Attn: SMTTM (LT C. Lee)
Air Force Unit Post Office
Los Angeles Air Force Station, CA 90045

Headquarters
Arnold Engineering Development Center
Attn: Library/Documents (Joe Ashley, Jr.)
R. W. Henzel, TD
DYR (CAPT C. Tirres)
Library/Documents
Arnold Air Force Station, TN 37389

von Karman Gas Dynamics Facility
ARO, Inc.
Attn: Dr. J. D. Whitfield, Chief
Arnold Air Force Station, TN 37389

Commanding Officer
Harry Diamond Laboratories
Attn: Library
Adelphi, MD 20783

Commanding General
U.S. Army Missile Command
Attn: AMSMI-RR
Chief, Document Section 2
AMSMI-RDK (R. A. Deep)
AMSMI-RDK (T. R. Street)
Redstone Arsenal, AL 35809

DISTRIBUTION (Cont.)

Department of the Army
Office of the Chief of Research and Development
ABMDA, The Pentagon
Washington, DC 20350

U.S. Army Cold Region Research and Engineering
Laboratory
Attn: Dr. Y. C. Yen
Hanover, NH 03755

Commanding Officer
Picatinny Arsenal
Attn: SMUPA-VC-3 (A. A. Loeb)
Dover, NJ 07801

Commander (ADL)
Naval Air Development Center
Warminster, PA 18974

Air Force Weapons Laboratory
Technical Library (SUL)
Kirtland Air Force Base
Albuquerque, NM 87117

U.S. Army Ballistic Missile Defense Agency
Attn: Dr. Sidney Alexander
1300 Wilson Boulevard
Arlington, VA 22209

Applied Physics Laboratory
Attn: Document Library 2
Dr. F. Hill
Dr. L. L. Cronvich
J. D. Randall
Johns Hopkins University
Johns Hopkins Road
Laurel, MD 20810

Director, Defense Nuclear Agency
Attn: STSP (SPAS) 2
Headquarters DASA
Washington, DC 20305

Commanding Officer
Naval Intelligence Support Center
4301 Suitland Road
Washington, DC 20390

DISTRIBUTION (Cont.)

Department of Aeronautics
Attn: COL D. H. Daley, Prof. & Head
DFAN
USAF Academy, CO 80840

Chief of Naval Research
Attn: ONR 100
Arlington, VA 22217

Air Force Armament Test Laboratory
Attn: C. B. Butler
Eglin Air Force Base, FL 32542

Headquarters, Edgewood Arsenal
Attn: A. Flateau
Edgewood Arsenal, MD 21010

Fluid Mechanics Research Laboratory
Wright-Patterson Air Force Base
Attn: E. G. Johnson, Director 5
Dayton, OH 45433

Commander
U.S. Army
Natick Laboratories
Attn: G. Barnard
STSNL-UBS
Natick, MA 01760

NASA Ames Research Center
Attn: Dr. M. Horstman
Mr. W. C. Davy
Moffett Field, CA 94035

Fluid Dynamics Laboratory
Wright-Patterson Air Force Base
Attn: Dr. D. J. Harney
Dayton, OH 45433

Energetics Laboratory
Wright-Patterson Air Force Base
Attn: Dr. A. W. Fiore
Dayton, OH 45433

Naval Postgraduate School
Attn: Prof. D. J. Collins
Department of Aeronautics
Monterey, CA 93940

DISTRIBUTION (Cont.)

University of Akron
Attn: Prof. B. T. F. Chung
Mechanical Engineering Department
Akron, OH 44325

Aerospace Engineering Program
University of Alabama
Attn: Prof. W. K. Roy, Chm.
P.O. Box 6307
Tuscaloosa, AL 35486

AME Department
University of Arizona
Attn: Dr. L. B. Scott
Tucson, AZ 85721

Polytechnic Institute of Brooklyn
Attn: Dr. J. Polczynski
Graduate Center Library
Route 110, Farmingdale
Long Island, NY 11735

Polytechnic Institute of Brooklyn
Attn: Reference Department
Spicer Library
333 Jay Street
Brooklyn, NY 11201

Brown University
Division of Engineering
Attn: Dr. M. Sibulkin
Library
Providence, RI 02912

California Institute of Technology
Attn: Graduate Aeronautical Laboratories
Aero. Librarian
Karman Lab-301 (Dr. H. Liepmann)
Firestone Flight Sciences Lab.
(Prof. L. Lees)
Guggenheim Lab. (Prof. D. Coles, 321)
Dr. A. Roshko
Pasadena, CA 91109

University of California
Attn: Dr. M. Holt
Dept. of Mechanical Engineering
Berkeley, CA 94720

DISTRIBUTION (Cont.)

University of California - Los Angeles
Attn: Prof. J. D. Cole
Dept. of Mechanics and Structures
Los Angeles, CA 90024

GASDYNAMICS
University of California
Attn: A. K. Oppenheim
Richmond Field Station
1301 South 46th Street
Richmond, CA 94804

Department of Aerospace Engineering
University of Southern California
Attn: Dr. John Laufer
University Park
Los Angeles, CA 90007

University of California - San Diego
Attn: Dr. P. A. Libby
Dr. H. K. Cheng
Department of Aerospace and Mechanical
Engineering Sciences
LaJolla, CA 92037

Case Western Reserve University
Attn: Dr. Eli Reshotko, Chairman
Department of Mechanical and
Aerospace Engineering
Cleveland, OH 44106

The Catholic University of America
Attn: Dr. C. C. Chang
Dr. Paul K. Chang,
Mechanical Engineering Dept.
Dr. M. J. Casarella,
Mechanical Engineering Dept.
Washington, DC 20017

University of Cincinnati
Attn: Department of Aerospace Engineering
Dr. Arnold Polak
Cincinnati, OH 45221

Department of Aerospace Engineering Sciences
University of Colorado
Boulder, CO 80302

DISTRIBUTION (Cont.)

Cornell University
Attn: Dr. S. F. Shen
Prof. F. K. Moore, Head
Thermal Engineering
Dept., 208 Upson Hall
Graduate School of Aero. Engineering
Ithaca, NY 14850

University of Delaware
Attn: Dr. James E. Danberg
Mechanical and Aeronautical Engineering Dept.
Newark, DE 19711

George Washington University
Attn: Prof. A. B. Cambel
Prof. R. Goulard
School of Engineering
Washington, DC 20052

Georgia Institute of Technology
Attn: Dr. Arnold L. Ducoffe
225 North Avenue, N.W.
Atlanta, GA 30332

Technical Reports Collection
Gordon McKay Library
Harvard University
Division of Engineering and Applied Physics
Pierce Hall
Oxford Street
Cambridge, MA 02138

Illinois Institute of Technology
Attn: Dr. M. V. Morkovin
Prof. A. A. Fejer, M.A.E. Dept.
3300 South Federal
Chicago, IL 60616

University of Illinois
Aeronautical and Astronautical Engineering
Department
101 Transportation Bldg.
Urbana, IL 61801

Iowa State University
Aerospace Engineering Dept.
Ames, Iowa 50010

DISTRIBUTION (Cont.)

The Johns Hopkins University
Attn: Professor S. Corrsin
Baltimore, MD 21218

University of Kentucky
Attn: C. F. Knapp
Wenner-Gren Aero. Lab.
Lexington, KY 40506

Department of Aero. Engineering, ME 106
Louisianna State University
Attn: Dr. P. H. Miller
Baton Rouge, LA 70803

University of Maryland
Attn: Prof. A. Wiley Sherwood,
Department of Aerospace Engineering
Prof. Charles A. Shreeve
Department of Mechanical Engineering
Dr. S. I. Pai, Institute for Fluid
Dynamics and Applied Mathematics
Dr. Redfield W. Allen, Department
of Mechanical Engineering
Dr. W. L. Melnik, Department of
Aerospace Engineering
Dr. John D. Anderson, Jr.
Department of Aerospace Engineering
College Park, MD 20740

Michigan State University
Attn: Library, Documents Department
East Lansing, MI 48823

Massachusetts Institute of Technology
Attn: Mr. J. R. Martucelli, Rm. 33-211
Prof. M. Finston
Prof. J. Baron, Dept. of Aero. and
Astro., Rm. 37-461
Prof. A. H. Shapiro, Head, Mech.
Engr. Dept.
Aero. Engineering Library
Prof. Ronald F. Probestein
Dr. E. E. Covert
Aerophysics Laboratory
Cambridge, MA 02139

DISTRIBUTION (Cont.)

University of Michigan
Attn: Dr. M. Sichel, Dept. of Aero. Engr.
Engineering Library
Aerospace Engineering Lib.
Mr. C. Cousineau, Engin-Trans Lib.
Dr. C. M. Vest, Dept. of Mech. Engr.
Ann Arbor, MI 48104

Serials and Documents Section
General Library
University of Michigan
Ann Arbor, MI 48104

Mississippi State University
Attn: Mr. Charles B. Cliett
Department of Aerophysics and
Aerospace Engineering
P.O. Drawer A
State College, MS 39762

U.S. Naval Academy
Engineering Department, Aerospace Division
Annapolis, MD 21402

U.S. Naval Postgraduate School
Library, Code 2124
Attn: Technical Reports Section
Monterey, CA 93940

New York University
Attn: Director of
Guggenheim Aerospace Laboratories
Prof. V. Zakkay
Engineering and Science Library
University Heights
New York, NY 10453

North Carolina State College
Attn: Dr. F. R. DeJarnette, Dept. Mech.
and Aero. Engineering
Dr. H. A. Hassan, Dept. of Mech.
and Aero. Engineering
Raleigh, NC 27607

North Carolina State University
Attn: D. H. Hill Library
P.O. Box 5007
Raleigh, NC 27607

DISTRIBUTION (Cont.)

University of North Carolina
Attn: Department of Aero. Engineering
Library, Documents Section
APROTC Det 590
Chapel Hill, NC 27514

Northwestern University
Technological Institute
Attn: Department of Mechanical Engineering
Library
Evanston, IL 60201

Notre Dame University
Attn: Dr. J. D. Nicolaides, Dept. of
Aero. Engineering
College of Engineering Library
South Bend, IN 46556

Department of Aero-Astro Engineering
Ohio State University
Attn: Engineering Library
Prof. J. D. Lee
Prof. G. L. Von Eschen
2036 Neil Avenue
Columbus, OH 43210

Ohio State University Libraries
Documents Division
1858 Neil Avenue
Columbus, OH 43210

The Pennsylvania State University
Attn: Dept. of Aero Engr., Hammond Bldg.
Library, Documents Section
University Park, PA 18602

Bevier Engineering Library
126 Benedum Hall
University of Pittsburgh
Pittsburgh, PA 15261

Princeton University
Attn: Prof. S. Bogdonoff
Dr. I. E. Vas
Aerospace & Mechanical Science Dept.
D-214 Engrg. Quadrangle
Princeton, NJ 08540

DISTRIBUTION (Cont.)

Purdue University
School of Aeronautical and Engineering
Sciences
Attn: Library
Dr. P. S. Lykoudis, Dept. of Aero.
Engineering
Lafayette, IN 47907

Rensselaer Polytechnic Institute
Attn: Dept. of Aeronautical Engineering
and Astronautics
Troy, NY 12181

Rutgers - The State University
Attn: Dr. R. H. Page
Dr. C. F. Chen
Department of Mechanical Industrial and
Aerospace Engineering
New Brunswick, NJ 08903

Stanford University
Attn: Librarian, Dept. of Aeronautics and
Astronautics
Stanford, CA 94305

Stevens Institute of Technology
Attn: Mechanical Engineering Department
Library
Hoboken, NJ 07030

The University of Texas at Austin
Attn: Engr S.B.114B, Dr. Friedrich
Applied Research Laboratories
P.O. Box 8029
Austin, TX 78712

University of Toledo
Attn: Dept. of Aero. Engineering
Dept. of Mech. Engineering
2801 W. Bancroft
Toledo, OH 43606

University of Virginia
School of Engineering and Applied Science
Attn: Dr. I. D. Jacobson
Dr. G. Matthews
Dr. R. N. Zapata
Charlottesville, VA 22901

DISTRIBUTION (Cont.)

University of Washington
Attn: Engineering Library
Dept. of Aeronautics and Astronautics
Prof. R. E. Street, Dept. of Aero. and Astro.
Prof. A. Hertzberg, Aero. and Astro., Guggeheim Hall
Seattle, WA 98105

West Virginia University
Attn: Library
Morgantown, WV 26506

Federal Reports Center
University of Wisconsin
Attn: S. Reilly
Mechanical Engineering Building
Madison, WI 53706

Los Alamos Scientific Laboratory
Attn: Report Library
P.O. Box 1663
Los Alamos, NM 87544

University of Maryland
Attn: Dr. R. C. Roberts,
Mathematics Department
Baltimore County (UMBC)
5401 Wilkens Avenue
Baltimore, MD 21228

Institute for Defense Analyses
Attn: Classified Library
400 Army-Navy Drive
Arlington, VA 22202

Kaman Sciences Corporation
Attn: Library
P.O. Box 7463
Colorado Springs, CO 80933

Kaman Science Corporation
Attn: Dr. J. R. Ruetenik
Avidyne Division
83 Second Avenue
Burlington, MA 01803

DISTRIBUTION (Cont.)

Rockwell International
B-1 Division
Technical Information Center (BA08)
International Airport
Los Angeles, CA 90009

Rockwell International Corporation
Technical Information Center
4300 E. Fifth Avenue
Columbus, OH 43216

M.I.T. Lincoln Laboratory
Attn: Library A-082
P.O. Box 73
Lexington, MA 02173

The RAND Corporation
Attn: Library - D
Dr. William S. King
1700 Main Street
Santa Monica, CA 90406

Aerojet Electrosystems Co.
Attn: Engineering Library
1100 W. Hollyvale Avenue
Azusa, CA 91702

The Boeing Company
Attn: 87-67
P.O. Box 3999
Seattle, WA 98124

United Aircraft
Research Laboratories
Attn: Dr. William M. Foley
East Hartford, CT 06108

United Aircraft Corporation
Attn: Library
400 Main Street
East Hartford, CT 06108

Hughes Aircraft Company
Attn: Company Tech. Doc. Center
6/E11, B. W. Campbell
Centinela at Teale
Culver City, CA 90230

DISTRIBUTION (Cont.)

Lockheed Missiles and Space Company, Inc.
Attn: Mr. G. M. Laden, Dept. 81-25,
Bldg. 154
Mr. Murl Culp
P.O. Box 504
Sunnyvale, CA 94086

Lockheed Missiles and Space Company
Attn: Technical Information Center
3251 Hanover Street
Palo Alto, CA 94304

Lockheed-California Company
Attn: Central Library, Dept. 84-40,
Bldg. 170
PLT. B-1
Burbank, CA 91503

Vice President and Chief Scientist
Dept. 03-10
Lockheed Aircraft Corporation
P.O. Box 551
Burbank, CA 91503

Martin Marietta Corporation
Martin Marietta Labs
Attn: Science-Technology Library
1450 S. Rolling Road
Baltimore, MD 21227

Martin Marietta Corporation
Orlando Division
P.O. Box 5837
Orlando, FL 32855

General Dynamics
Attn: Research Library 2246
George Kaler, Mail Zone 2880
P.O. Box 748
Fort Worth, TX 76101

Calspan Corporation
Attn: Library
4455 Genesee Street
Buffalo, NY 14221

Air University Library
(SE) 63-578
Maxwell Air Force Base, AL 36112

DISTRIBUTION (Cont.)

McDonnell Company
Attn: R. D. Detrich, Dept. 209,
Bldg. 33
P.O. Box 516
St. Louis, MO 63166

McDonnell-Douglas Aircraft Corporation
Missile and Space Systems Division
Attn: A2-260 Library
Dr. J. S. Murphy, A-830
Mr. W. H. Branch, Director
300 Ocean Park Boulevard
Santa Monica, CA 90405

Fairchild Industries, Inc.
Fairchild Republic Co.
Attn: Engineering Library
Conklin Street
Farmingdale, NY 11735

General Applied Science Laboratories, Inc.
Attn: Dr. F. Lane
Merrick and Stewart Avenues
Westbury, Long Island, NY 11590

General Electric Company
Attn: Dr. H. T. Nagamatsu
Research and Development Lab. (Comb. Bldg.)
Schenectady, NY 12301

The Whitney Library
General Electric Research and Development Center
Attn: M. F. Orr, Manager
The Knolls, K-1
P.O. Box 8
Schenectady, NY 12301

General Electric Company
Missile and Space Division
Attn: MSD Library
Larry Chasen, Mgr.
Dr. J. D. Stewart, Mgr.
Research and Engineering
P.O. Box 8555
Philadelphia, PA 19101

General Electric Company
AEG Technical Information Center, N-32
Cincinnati, OH 45215

DISTRIBUTION (Cont.)

General Electric Company
Missile and Space Division
Attn: Dr. S. M. Scala
Dr. H. Lew
Mr. J. W. Faust
A. Martellucci
W. Daskin
J. D. Cresswell
J. B. Arnaiz
L. A. Marshall
J. Cassanto
R. Hobbs
C. Harris
F. George
P.O. Box 8555
Philadelphia, PA 19101

AVCO-Everett Research Laboratory
Attn: Library 2
Dr. George Sutton
2385 Revere Beach Parkway
Everett, MA 02149

Vought Corporation
P.O. Box 225907
Dallas, TX 75265

Northrop Corp.
Electronic Division
2301 W. 120th Street
Hawthorne, CA 90250

Government Documents
The Foundren Library
Rice Institute
P.O. Box 1892
Houston, TX 77001

Grumman Aerospace Corporation
Attn: Mr. R. A. Scheuing
Mr. H. B. Hopkins
Mr. H. R. Reed
South Oyster Bay Road
Bethpage, Long Island, NY 11714

The Marquardt Company
P.O. Box 2013
Van Nuys, CA 91409

DISTRIBUTION (Cont.)

ARDE Associates
Attn: Librarian
P.O. Box 286
580 Winters Avenue
Paramus, NJ 07652

Aerophysics Company
Attn: Mr. G. D. Boehler
3500 Connecticut Avenue, N.W.
Washington, DC 20003

Aeronautical Research Associates
of Princeton
Attn: Dr. C. duP. Donaldson
50 Washington Road
Princeton, NJ 08540

General Research Corporation
Attn: Technical Information Office
5383 Hollister Avenue
P.O. Box 3587
Santa Barbara, CA 93105

Sandia Laboratories
Attn: Mr. K. Goin, Div. 5642
Mrs. B. R. Allen, 3421
Mr. W. H. Curry, 5625
Mr. A. M. Torneby, 3141
Dr. C. Peterson
Box 5800
Albuquerque, NM 87115

Hercules Incorporated
Attn: Library
Allegany Ballistics Laboratory
P.O. Box 210
Cumberland, MD 21502

General Electric Company
Attn: Dave Hovis, Rm. 4109
P.O. Box 2500
Daytona Beach, FL 32015

TRW Defense & Space Systems Group
Attn: Technical Libr/Doc Acquisitions
Dr. A. B. Witte
One Space Park
Redondo Beach, CA 90278

DISTRIBUTION (Cont.)

Stanford Research Institute
Attn: Dr. G. Abrahamson
333 Ravenswood Avenue
Menlo Park, CA 94025

Hughes Aircraft Company
Attn: Technical Library, 600-C222
P.O. Box 3310
Fullerton, CA 92634

Westinghouse Electric Corporation
Astronuclear Laboratory
Attn: Library
P.O. Box 10864
Pittsburgh, PA 15236

University of Tennessee
Space Institute
Attn: Prof. J. M. Wu
Tullahoma, TN 37388

CONVAIR Division of General Dynamics
Library and Information Services
P.O. Box 12009
San Diego, CA 92112

CONVAIR Division of General Dynamics
Attn: Dr. J. Raat, Mail Zone 640-02
P.O. Box 80847
San Diego, CA 92138

AVCO Missiles Systems Division
Attn: E. E. H. Schurmann
J. Otis
201 Lowell Street
Wilmington, MA 01887

Chrysler Corporation
Space Division
Attn: G. T. Boyd, Dept. 2781
E. A. Rawk, Dept. 2920
P.O. Box 29200
New Orleans, LA 70129

General Dynamics
Pomona Division
Attn: Tech. Doc. Center, Mail Zone 6-20
P.O. Box 2507
Pomona, CA 91766

DISTRIBUTION (Cont.)

General Electric Company
Attn: W. Danskin
Larry Chasen
Dr. H. Lew
3198 Chesnut Street
Philadelphia, PA 19101

Ford Aerospace & Communication Corporation
Attn: Dr. A. Demetriades
Ford and Jamboree Roads
Newport Beach, CA 92663

Raytheon Company
Attn: D. P. Forsmo
Missile Systems Division
Hartwell Road
Bedford, MA 01730

TRW Systems Group
Attn: M. W. Sweeney, Jr.
Space Park Drive
Houston, TX 77058

Marine Bioscience Laboratory
Attn: Dr. A. C. Charters
513 Sydnor Street
Ridgecrest, CA 93555

University of Wyoming
Attn: Head, Dept. Mech. Eng.
University Station
P.O. Box 3295
Laramie, WY 82070

Applied Mechanics Review
Southwest Research Institute
8500 Culebra Road
San Antonio, TX 78228

American Institute of Aeronautics
and Astronautics
Attn: J. Newbauer
1290 Sixth Avenue
New York, NY 10019

DISTRIBUTION (Cont.)

Technical Information Service
American Institute of Aeronautics and
Astronautics
Attn: Miss P. Marshall
750 Third Avenue
New York, NY 10017

Faculty of Aeronautical Systems
University of West Florida
Attn: Dr. R. Fledderman
Pensacola, FL 32504

Saber Industries, Inc.
Attn: J. A. Finkel
Library
P.O. Box 60
North Troy, VT 05859

Pratt and Whitney Aircraft
Attn: W. G. Alwang, EB-1M5
East Hartford, CT 06108

Science Applications, Inc.
Attn: Dr. J. D. Trolinger
P.O. Box 861
Tullahoma, TN 37388

The Aerospace Corporation
Attn: J. M. Lyons, Bldg. 82
P.O. Box 92957
Los Angeles, CA 90009

NDW-NSWC(W)-5605/1 (Rev. 5-78)

TO AID IN UPDATING THE DISTRIBUTION LIST FOR NAVAL SURFACE WEAPONS CENTER, WHITE OAK TECHNICAL REPORTS PLEASE COMPLETE THE FORM BELOW:

TO ALL HOLDERS OF NSWC/TR 79-139
by T. F. Zien, Code R-44
DO NOT RETURN THIS FORM IF ALL INFORMATION IS CURRENT

A. FACILITY NAME AND ADDRESS *(OLD) (Show Zip Code)*

NEW ADDRESS *(Show Zip Code)*

B. ATTENTION LINE ADDRESSES:

C.

☐ REMOVE THIS FACILITY FROM THE DISTRIBUTION LIST FOR TECHNICAL REPORTS ON THIS SUBJECT.

D.
NUMBER OF COPIES DESIRED _____

GPO 930-784

DEPARTMENT OF THE NAVY
NAVAL SURFACE WEAPONS CENTER
WHITE OAK, SILVER SPRING, MD. 20910

OFFICIAL BUSINESS
PENALTY FOR PRIVATE USE, $300

POSTAGE AND FEES PAID
DEPARTMENT OF THE NAVY
DOD 316

COMMANDER
NAVAL SURFACE WEAPONS CENTER
WHITE OAK, SILVER SPRING, MARYLAND 20910

ATTENTION: CODE R-44


D'A
FIL
5